INDC

INTERNATIONAL NUCLEAR DATA COMMITTEE

Neutron Cross-Sections of Deuterium in the Energy

Range 0.0001 eV-15 MeV

N.O. Bazazyants, A.S. Zabrodskaya

A.F. Larina, M.N. Nikolaev

Neutron Cross-Sections of Deuterium in the Energy

Range 0.0001 eV-15 MeV

N.O. Bazazyants, A.S. Zabrodskaya

A.F. Larina, M.N. Nikolaev

NEUTRON CROSS-SECTIONS OF DEUTERIUM IN THE ENERGY
RANGE 0.0001 eV-15 MeV

N.O. Bazazyants, A.S. Zabrodskaya
A.F. Larina, M.N. Nikolaev

ABSTRACT

The paper describes the evaluation of deuterium neutron cross-sections, the spectra of neutrons from the reaction $D(n,2n)P$ and the angular distributions of neutrons from this reaction and of neutrons elastically scattered on deuterium.

The evaluation results are presented in the SOCRATOR format. The 26-group system of constants for deuterium is also presented.

Introduction

In the evaluations of deuterium neutron cross-sections performed by Horsley [1] in 1965-67 and by Leonard in 1972 (the latter evaluation served as the basis for the set of neutron data for deuterium in the second version of ENDF/B), considerable discrepancies were noted between the results obtained with different experimental data on the deuterium scattering cross-section in the low-energy region. Judging by the brief description of the 1973 neutron cross-section evaluation for the third version of ENDF/B [27], the discrepancies were apparently not resolved in this evaluation either.

In our opinion, the new experimental data of recent times [P-15, P-16, T-9] offer the possibility of resolving the discrepancies and of choosing with far better justification the total cross-section of deuterium in the low-energy region. Accordingly, the decision was taken to re-evaluate the cross-sections of deuterium for SOCRATOR. The present paper describes the re-evaluation and discusses the results.

The references used are presented with brief annotations in: Table 3 - data on the energy dependence of the total cross-section in the fast-neutron region (references prefaced by the letter "P"); Table 4 - data on cross-sections for the scattering of slow neutrons (references prefaced by the letter "T"); Table 5 - data on the angular distribution of elastically scattered neutrons (references prefaced by the letter "E"); Table 6 - data on the cross-section for the reaction (n,2n) (references prefaced by the letter "N"). References to information sources not included in these tables are presented in the list at the end of the paper.

In accordance with Ref. [25], the mass of deuterium (or the $A(^{12}C) = 12$ scale) is taken to be 2.0141022. The binding energy of a deuteron is taken to be 2.225 MeV [26]; the spin I = 1.

Only three neutron-deuterium interactions are possible at energies below 15 MeV:

1. Elastic scattering;

2. Radiative capture;

3. The reaction (n,2n).

The cross-sections for these reactions and the total cross-section for the interaction of neutrons with deuterium nuclei are discussed below. Deuterium cross-sections are considered in this paper only for unbound atoms.

1. Total cross-section

Figures 1a and 1b show the results of deuterium total cross-section measurements performed between 1946 and the present. For energies above 0.5 MeV, the energy dependence of the total cross-section was established with a comparatively high degree of accuracy by Seagrave and Henkel [P-9] in 1955, Bratenahl et al. [P-10] in 1958 and Willard et al. [P-11] in 1964 (Table 3). Later, the data of these authors were confirmed by the measurements of Glasgow and Foster [P-12] in 1967 and Davis and Barschall [P-13] in 1971.

For energies below 0.5 MeV, the energy dependence of the cross-section was usually obtained by extrapolating the data of Seagrave and Henkel [P-9], which extended to 0.27 MeV, to lower energies. In this extrapolation, no account was taken of the results reported by Allen et al. [P-8] in 1955, which pointed to a major increase in the total cross-section as one moved from 0.2 MeV to 0.1 MeV, or of the very dispersed data of earlier works: [P-1], 1946; [P-5], 1953; [P-6], 1953; [P-7], 1953 (see Fig. 1b).

In 1972 there appeared two works by a group of authors from Rensselaer Polytechnic Institute - P. Stoler et al. [P-14 and P-15] - in which systematic total cross-section measurements were made with an accuracy of ~ 1% for the energy ranges from ~ 0 to 1 MeV [P-15] and from ~ 0.5 MeV to 30 MeV [P-14]. According to Ref. [P-15], the energy dependence of the total cross-section falls sharply (from σ_t = 3.4 barn to σ_t = 3.1 barn) in the range ~ 0-200 keV.

The continuous curve in Fig. 1b shows the results of theoretical calculations [4] presented in Ref. [P-15]. The rapid decrease in the cross-section is attributable to the prevalence of the S-wave in this region and the smooth dependence above 200 keV to the early appearance of higher moments of scattering caused by the large radius of deuterium. This is the reason for the difference between the energy dependence of the total cross-section of deuterium and the cross-section of hydrogen, for which S-scattering dominates right up to 10 MeV. With the results of P. Stoler et al. [P-15] it has been possible to resolve the contradiction in the data on the value of the deuterium cross-section in the low-energy region. This contradiction is explained below.

Direct measurements of the cross-section for the scattering of slow neutrons on free deuterium nuclei yielded results such as the following (see Table 4):

3.44 ± 0.06 barn, Fermi and Marshall [T-1], 1949;

3.4 ± 0.4 barn, Hurst and Alcock [T-3], 1951;

3.390 ± 0.012 barn, Dilg et al. [T-9], 1971.

The value recommended in BNL-325 is 3.38 ± 0.05 barn [3].

The cross-section for scattering on free deuterium is linked with the doublet $(Y = \frac{1}{2})$ - a_2 - and quartet $(y = \frac{3}{2})$ - a_4 - scattering lengths by the relation

$$\sigma_{free} = 4\pi \left(\frac{2}{3} a_4^2 + \frac{1}{3} a_2^2\right).$$

By measuring the coherent scattering cross-section $\sigma_{coh} = 4\pi \left(a_4 + \frac{1}{2}a_2\right)^2$ or the incoherent scattering cross-section $\sigma_{incoh} = 2\pi\left(a_4 - a_2\right)^2$ for a known σ_{free}, it is possible to determine a_4 and a_2 separately if one has an idea which of them is greater.

The data of I.A. Ivanenko et al. [T-8] on the interaction of polarized neutrons with polarized deuterium nuclei definitely indicate that $a_4 > a_2$.

The cross-section for incoherent scattering has been measured only by
V.W. Gissler [T-5], who has obtained

$$\sigma_{coh} = 2.25 \pm 0.04 \text{ barn,}$$

from which $a_4 - a_2 = 6.0 \pm 0.2$ F.

Measurements of the coherent scattering cross-section for $a_4 + a_2/2$
have yielded the following results:

6.4 $\pm$ 0.2 F, C.G. Shull and E.O. Wallen [T-2], 1951;

6.70 $\pm$ 0.05 F, L. Koester and H. Ungerer [T-6], 1969;

6.21 $\pm$ 0.04 F, W. Bartolini et al. [T-7], 1968;

6.67 $\pm$ 0.02 F, W. Dilg et al. [T-9], 1971.

The obvious discrepancy between the data of Bartolini [T-7] and of Dilg [T-9],
which are in agreement with those of Koester and Ungerer [T-6], needed to be
resolved.

If one takes Bartolini's low value of a_{coh}, the values of ~ 3.4 barn
for σ_{free} cannot be reconciled with the conclusion that $a_4 > a_2$ [T-8].
This difficulty can be overcome by taking a lower value of σ_{free}. Further
justification was provided by the data of Seagrave [P-10], who measured the
total cross-section of deuterium in the energy range 0.267-4.002 MeV and
above. Seagrave's data are extrapolated into the low-energy region to
σ_{free} ~ 3.1-3.2 barn. This obliged A. Horsley [1], in evaluating the cross-
sections of deuterium, to take σ_{free} = 3.15 barn. Such a result can be
reconciled with the data of Bartolini et al. [T-7] and Ivanenko et al. [T-8]
for $a_2 > 0$*/; however, the relation a_2/a_4 = 0.04 following from these data
differs very much from the experimental values: 0.12 $\pm$ 0.04 barn [T-3]
and 0.08 $\pm$ 0.03 barn [T-4]. This discrepancy has been pointed out by
B.R. Leonard [2], who performed a deuterium cross-section evaluation for
ENDF/B-II. Leonard also noted that, for σ_{free} = 3.5 barn, it is impossible
to explain the experimental data for the age of neutrons in heavy water.
In order to eliminate the discrepancies in the calculated and experimental
age values, Leonard took σ_{free} = 3.35 barn. Soon after the publication of
Leonard's work [2], Dilg et al. [T-8] reported on the results of very careful
measurements of σ_{free} and a_{coh} for deuterium. It is difficult to fault the

---

*/ Translator's note - Original not clear.

methodic purity of the results of this work. However, the value of σ_{free} obtained, 3.390 $\pm$ 0.012 barn, contradicts the extrapolation of Seagrave's data. At the same time, the scattering length values a_4 = 6.35 $\pm$ 0.02 F and a_2 = 0.65 $\pm$ 0.04 F which follow from Dilg's work are in excellent agreement with the data of most other authors (except Bartolini et al. [T-7]). The data obtained by P. Stoler et al. [P-15] showed that extrapolation of the cross-sections measured by Seagrave to the low-energy region was done incorrectly. In actual fact, owing to the rapid decline in the contribution of the S-wave, the total cross-section of deuterium declines sharply as one moves from the slow-neutron region to an energy of ~ 0.2 MeV.

Thus, the contradiction between the data on total cross-sections in the region from hundreds of keV to 1 MeV (including Seagrave's data) and the data for slow neutrons has been eliminated. The values for deuterium cross-sections at low energies taken in this work are based completely on the measurements of Dilg [T-9] and Stoler [P-15]:

$$a_2 = 0.65 \text{ F};$$

$$a_4 = 6.35 \text{ F};$$

$$\sigma_{free} (E \to 0) = 3.39 \text{ barn}.$$

Let us now consider the basic works in which the total cross-section of deuterium for the intermediate-energy range was measured. The first of these, in chronological order, is the work of Seagrave and Henkel [P-9] performed in 1955. Data were obtained for neutrons with energies in the range 0.3-22 MeV. A gaseous sample under high pressure was used for the measurements; unfortunately, the experimental points are very scattered, and in the energy regions from 1.4 MeV to 4.2 MeV and from 8 MeV to 14 MeV there are no data at all. Later, Glasgow and Foster [P-12] measured the total cross-section of deuterium using a continuous neutron spectrum; they employed the time-of-flight method, the measurement accuracy was 1-5% and data were obtained for 241 energy values in the range 2.25-15.0 MeV. In 1971, Davis and Barschal [P-13] published the results of $\sigma_t(D)$ measurements performed at energies in the range 1.5-26 MeV with an accuracy of 1-2%; below 3 MeV they are in agreement with the results of Seagrave and Henkel [P-9] and above 3 MeV in agreement with the data of Glasgow and Foster [P-12]. Lastly, in 1972, Clement et al. [P-14] measured the total cross-section of

deuterium in the energy region 0.52-30 MeV to within 1%. The measurements
were so detailed that we have included in the figure[*] points which are the
result of averaging experimental data with intervals of 0.1 MeV (from
0.52 MeV to 2 MeV), 0.125 MeV (from 2.0 MeV to 10 MeV) and 0.25 MeV (from
10 MeV to 15 MeV). The results of this work are in good agreement with
the data of Seagrave and Henkel. We would point out that a pure gaseous
deuterium target was used in both works. In two other series of measurements
(Glasgow and Foster [P-12], Davis and Barschall [P-13]), the target was
hydrocarbonate enriched in deuterium, so that it was necessary to subtract
the carbon cross-section and additional errors consequently arose.

In the region ~ 0.5-1 MeV, the data of Stoler et al. [P-15] and those
of Clement et al. [P-14] are in excellent agreement both among themselves
and with the curve computed in Ref. [4], which tends to 3.39 barn as $E \to 0$
in accordance with the results of Dilg [T-9].

In this evaluation, therefore, in the region from 1 eV to 1 MeV the
total cross-section of deuterium is in accordance with the data of the
three above-mentioned works (the recommended curve coincides with the curve
in Ref. [P-15]), while from 1 MeV to 15 MeV it is in accordance with the
data of Clements et al. [P-14].

For E = 130 eV and for lower energies,

$$\sigma_t = 3.39 + \sigma_{n\gamma} \text{ barn.}$$

Let us now consider the question of the accuracy of the evaluated total
cross-sections. Specifying the accuracy of a cross-section $\sigma(E)$ means
specifying the parameters of the algorithm by means of which, for any E
and E' lying in the energy region under consideration, it is possible to
determine the correlation function

$$g(E,E') = \overline{\delta\sigma(E) \cdot \delta\sigma(E')},$$

where $\delta\sigma(E)$ is the deviation of the evaluated cross-section from the true
one and the line denotes averaging over all possible deviations with the
probability density of these deviations as the weighting function.

If g(E,E') is known, with it one can easily calculate the covariance
matrix of the group cross-sections:

$$\sigma_g = \frac{1}{\Delta E_g} \int_{\Delta E_g} \sigma(E) \, \psi_g(E) \, dE,$$

---

[*] Translator's note - Which figure?

where $\mathcal{J}g(E)$ is the intragroup spectrum normalized to ΔEg. In fact,

$$\overline{\delta\sigma_g \cdot \delta\sigma_{g'}} = \frac{1}{\Delta E_g \Delta E_{g'}} \int\limits_{\Delta E_g} dE \int\limits_{\Delta E_{g'}} dE' \cdot g(E,E') \mathcal{J}_g(E) \mathcal{J}_g(E').$$

Let us assume that the energy region 0-15 MeV is broken down by E_i points, $i = 0,1,\ldots.n$, $(E_0 = 0, E_n = 15$ MeV$)$, in such a way that the cross-section errors can be considered fully correlated at points $E_0 = 0$ and E_1 and fully uncorrelated at the remaining points:

$$\overline{\delta\sigma(0)\,\delta\sigma(E_1)} = \overline{\delta^2\sigma_1} ;$$

$$\overline{\delta\sigma(E_i) \cdot \delta\sigma(E_k)} = \overline{\delta^2\sigma_i} \cdot \delta_{ik} \qquad (i,k = 1,2,\ldots, n).$$

Here δ_{ik} is the Kronecker symbol.

Let us also assume that, in the ranges $[E_{i-1}, E_i]$, the energy dependence of the total cross-section can be presented in the form

$$\sigma(E) = a + b \cdot E + \Delta\sigma(E),$$

where $\Delta\sigma(E) \ll \sigma(E)$.

In this case, ignoring the fact that the correction function $\Delta\sigma(E)$ is not known accurately, we obtain

$$g(E,E') \left\{ \begin{array}{ll} \overline{\delta^2\sigma_1}, & (E, E' \in [0, E_1]) \\[2ex] \overline{\delta^2\sigma_1}\, \dfrac{E_2 - E'}{E_2 - E_1}, & (E \in [0, E_1], E' \in [E_1, E_2]) \end{array} \right.$$

and, for $i = 2, \ldots, n$,

$$g(E,E') \left\{ \begin{array}{ll} \overline{\delta^2\sigma_{i-1}}\, \dfrac{(E_i - E)(E_i - E')}{(E_i - E_{i-1})^2} + \overline{\delta^2\sigma_i}\, \dfrac{(E - E_{i-1})(E' - E_{i-1})}{(E_i - E_{i-1})^2}, & (E, E' \in [E_{i-1}, E_i]) \\[2ex] \overline{\delta^2\sigma_i} \cdot \dfrac{(E - E_{i-1})(E_{i+1} - E')}{(E_i - E_{i-1})(E_{i+1} - E_i)}, & (E \in [E_{i-1}, E_i], E' \in [E_i, E_{i+1}]) \\[2ex] 0, & (E < E_{i-1}, E' > E_i). \end{array} \right.$$

Thus, $g(E,E')$ can be specified by the parameters E_i and $\overline{\delta^2\sigma}_i \equiv \overline{\delta^2\sigma(E_i)}$, $i = 1, \ldots, n$.

Let us now try to choose the corresponding values of E_i and estimate[*]/ $\delta^2\sigma_i$.

In the energy region 10^{-4} eV–10 keV, the total cross-section of deuterium is constant to within well under 1%. The evaluated cross-section for scattering in this region is completely determined by the result of Dilg et al. [T-9] obtained with an accuracy of 0.35%. As there is only one result having such a high degree of accuracy, the uncertainty associated with the total cross-section at energies below 10 keV should, in our opinion, be taken to be somewhat higher: 0.5%. Thus, $E_1 = 0.01$ MeV and $\frac{1}{\sigma_1}\sqrt{\delta^2\sigma_1} = 0.005$. It is best to take the boundary of the following interval to be 0.2 MeV. The energy dependence of the cross-section in the 10–200 keV range is determined completely by the data of Stoler et al. [P-15]. The non-linearity in this range is of the order of 1%.

The accuracy of the evaluated cross-section at 0.2 MeV is ~ 1% (that is the accuracy of the data in Ref. [P-15], which agree with the result of Seagrave and Henkel at 0.27 MeV with an accuracy of ~ 1.5%; see Fig. 1b). The error associated with the cross-section at this energy in no way correlates with the value of the cross-section at low energies.

Thus, $E_2 = 0.2$ MeV and $\frac{1}{\sigma_2}\sqrt{\delta^2\sigma_2} = 0.01$. It is best to extend the third range to 4 MeV. In this case, the non-linearity of the energy dependence of the cross-section will be 2–3%. In the vicinity of 4 MeV, the estimated cross-section value is confirmed by a number of results (see Fig. 1a) which agree among themselves within the limits of errors amounting to 1.5–5%. The accuracy which we ascribe to the result for 4 MeV is 1.5%. For all practical purposes, this error does not correlate with the error at ~ 0.2 MeV as the sets of results determining the cross-sections at these energy points hardly overlap. Thus, $E_3 = 4$ MeV and $\frac{1}{\sigma_3}\sqrt{\delta^2\sigma_3} = 0.015$.

The region above 4 MeV is combined into one last energy range. The non-linearity from 4 MeV to 15 MeV is 5–7%, but that is acceptable for estimating errors. The error in the estimated cross-section at 14–15 MeV appears to be ~ 4% (on the basis of the spread of the data of different authors). Because of the considerable difference between the accuracies of the estimated cross-section at 4 MeV and 15 MeV, the correlations between them may be ignored despite the fact that, at both energies, the choice of

---

[*]/ Translator's note – The Russians use one word to mean both "estimate" and "evaluate".

evaluated cross-sections is made mainly on the basis of data from only two works [P-12 and P-14]. The error increase as one goes to 15 MeV indicated that, with rising energy, there appears an additional source of error which is decisive at 15 MeV. This is what justifies ignoring the correlations between $\delta\sigma_3$ and $\delta\sigma_4$. Thus, E_4 = 15 MeV and $\frac{1}{\sigma_4}\sqrt{\delta^2\sigma_4}$ = 0.04.

The results of the estimate of the errors in the total cross-section of deuterium are summarized in Table 1.

Table 1

Errors in the total cross-section of deuterium

i – number of range	E_i (MeV) – upper energy limit	$\max\left\{\frac{\Delta\sigma(E)}{\sigma(E)}\right\}$ %	$\frac{1}{\sigma_i}\sqrt{\delta^2\sigma_i}$
1	0.01	< 1	0.005
2	0.2	~ 1	0.010
3	4.0	2-3	0.015
4	15.0	5-7	0.04

With regard to the calculation of the correlation properties of the errors, see the text.

2. Cross-section for radiative capture

The radiative capture cross-section (see Fig. 2) of deuterium is taken to be in accordance with the evaluation of Horsley [1]. There is a scarcity of experimental data on the cross-section for the capture of thermal neutrons by deuterium:

521 ± 9 µbarn, J.S. Merritt et al. [5], 1968;

506 ± 10 µbarn, J.S. Merritt et al. [6], 1967;

600 ± 50 µbarn, E.T. Jurney and H.T. Motz [7], 1963;

570 ± 10 µbarn, L. Kaplan et al. [8], 1952.

The later result of Merritt et al. [5], which differs somewhat from their earlier one [6] but is more accurate, is taken as the recommended value for $\sigma_{n\gamma}$ at 0.0253 eV. In the high-energy region, the value taken for the capture cross-section is that of Horsley in accordance with a recalculation on the basis of a detailed balance of data on the cross-section

for the reverse reaction $T(\gamma,n)D$ measured by R. Bösch et al. [9] and
R. Kosiek et al. [10]. The recalculation was performed using a modification
of the theory of J.C. Gunn and J. Irving [11], which enables one to describe
the photodecay of three-nucleon systems. Despite the improvements made,
the theory does not describe the behaviour of the capture cross-section
in the low-energy region. The matching of data for high energies and at
the thermal point is performed according to the $^1/v$ law. It should be noted
that the cross-section for capture at 14 MeV taken on the basis of the detailed
balance principle (9.5 μbarn) does not agree with the results of direct
measurements of this cross-section performed by the Zagreb group (see
Refs [12] (29.4 ± 5.8 μbarn) and [13] (31.6 ± 1.8 μbarn)).

The accuracy of the capture cross-section at the thermal point is 2%.
This degree of accuracy is retained wherever the cross-section clearly obeys
the $^1/v$ law, i.e. as far as 1 keV, the cross-section errors in this region
being very closely correlated:

$$\overline{\delta\sigma_\gamma(E)\cdot\delta\sigma_\gamma(E')} = \frac{\overline{\delta\sigma_\gamma^2(0.025\,\text{eV})}}{\sigma_\gamma^2(0.025\,\text{eV})} \quad \sigma_\gamma(E)\cdot\sigma_\gamma(E') =$$

$$= 4\cdot10^{-4}\cdot\sigma_\gamma(E)\cdot\sigma_\gamma(E') \qquad (E,E' < 1\ \text{keV}).$$

At energies above 100 keV, where the cross-section is estimated on the basis
of recalculation from the energy dependence of the cross-section for the
reverse reaction and where the estimate differs very much from the results
of direct measurements, the uncertainty associated with the capture cross-
section is — in our opinion — not less than 100%; here also the errors
must be considered fully correlated:

$$\overline{\delta\sigma_\gamma(E)\cdot\delta\sigma_\gamma(E')} = \sigma_\gamma(E)\cdot\sigma_\gamma(E') \qquad (E,E' > 100\ \text{keV}).$$

In the intermediate energy region,

$$\overline{\delta\sigma_\gamma(E)\cdot\delta\sigma_\gamma(E')} = 0.3\cdot10^{-16}(10-E)(10-E') + 0.5\cdot10^{-13}(E-1)(E'-1)$$
$$(1 \le E, E' \le 100\ \text{keV});$$

$$\overline{\delta\sigma_\gamma(E)\cdot\delta\sigma_\gamma(E')} = 2.5\cdot10^{-16}(10-E') \qquad (E<1\ \text{keV}; 1\le E' \le 100\ \text{keV});$$

$$\overline{\delta\sigma_\gamma(E)\cdot\delta\sigma_\gamma(E')} = 0.4\cdot10^{-12}(E-1) \qquad (1 \le E \le 100\ \text{keV}; E' > 100\ \text{keV}).$$

Cross-section for scattering

At energies below 130 eV, σ_e is taken to be 3.39 barn. In the energy range from 130 eV to the $(n,2n)$ reaction threshold, i.e. to 3.339 MeV, $\sigma_e = \sigma_t - \sigma_\gamma$. At higher energies, $\sigma_e = \sigma_t - \sigma_\gamma - \sigma_{2n}$.

The accuracy of the estimated elastic scattering cross-section values is therefore determined by the accuracy of the total cross-section and, above 3.4 MeV, the accuracy of the $(n,2n)$ reaction cross-section (the error in σ_γ has virtually no effect on the accuracy of σ_e).

4. Angular distributions of elastically scattered neutrons

For convenience in taking into account their energy dependences, the angular distributions of elastically scattered neutrons are represented in the form of expansions in Legendre polynomials:

$$\sigma_e(E,\mu) = \frac{1}{4\pi} \sum_{l=0}^{\lambda} B_l(E) \cdot P_l(\mu) = \frac{\sigma_e(E)}{4\pi} \sum_{l=0}^{\lambda} W_l(E) \cdot P_l(\mu),$$

where

$$W_l(E) = B_l(E) / B_0(E);$$

$$B_0(E) = \sigma_e(E).$$

An estimate of the energy dependences $B_l(E)$ was made by us earlier [14] on the basis of data published up to the middle of 1967. The results of this estimate are presented in numerical form in Ref. [15]. Meanwhile, some additional experimental information has been published on the angular distributions of neutrons elastically scattered on deuterium [E-8, E-9, E-12, E-13]. Thanks to these data and to the results of measurements of the angular distributions of proton scattering on deuterium nuclei [28-32], it has been possible to increase considerably the reliability of the estimate of the coefficients of expansion in Legendre polynomials at energies above 3 MeV and to represent the accuracy of the estimate.

The bibliographical information about experimental work relating to the elastic scattering of neutrons or deuterium is brought together in Table 5, where the main characteristics of the experiments are presented.

Figs 3a and 3b show the energy dependences of the $\omega_l(E)$ expansion coefficients. The points indicate results obtained by the least squares

method from experimental angular distributions (see Ref. [14]). The energy
dependence of the elastic scattering cross-section is also presented in
Figs 3a and 3b.

In Figs 4a-e, the angular distributions reconstructed on the basis of
estimated energy dependences of B_ℓ are compared with experimental data.

When expanding individual angular distributions in Legendre polynomials
by the least squares method, one may find not only expansion coefficients
but also the total covariance matrix of their errors. The expansion
coefficient accuracies determined in this way are always high (%) and
fairly strongly correlated; at the same time, the absolute errors in ω_ℓ
are only slightly dependent on ℓ. It can be seen from Fig. 3 that the
results of different authors differ among themselves and from the estimated
smooth $\omega_\ell(E)$ curves by much more than the errors estimated in treating
individual angular distributions, i.e. without allowance for the requirement
that the $\omega_\ell(E)$ energy dependences be smooth. This indicates that sources
of systematic errors not identified by the authors are the factors determining
the accuracy of the experimental results. The reasons for the discrepancies
cannot be discovered on the basis of published information about the experi-
mental conditions. Consequently, the recommended curve was drawn smoothly
among all the experimental points and the spread of the points relative to
this curve is a measure of its accuracy. As can be seen from Fig. 3, there
are no marked correlations among the deviations of the experimental points
from the smooth energy dependence $\sigma_\ell(E)$, $\omega_1(E)$, $\omega_2(E)$, etc. Hence, the
errors in $\omega_\ell(E)$ estimated from the spread of the points may be regarded as
uncorrelated among themselves and with the errors in the scattering cross-
section. For estimating the influence of the accuracy with which the angular
distributions are known on the neutron calculation results it is, as a rule,
sufficient to know the accuracy with which the mean cosine of the scattering
angle, $\mu = \omega_1/3$, is known. We shall therefore confine ourselves to estimating
the accuracy of this quantity.

At zero neutron energy, the scattering of neutrons on free deuterium
nuclei in the centre-of-mass system is clearly isotropic. Hence, $\delta^2\omega_1 = 0$
as $E \to 0$. In the 0.5 MeV region, the error in ω_1 appears to be about 50%.
Judging by the spread of the data in Refs [E-2], [E-4], [E-5] and [E-7], at
2-3 MeV the error declines to $\lesssim$ 30%.

The accuracy with which ω_1 is known at this energy may be regarded as uncorrelated with the errors in the estimated values of the mean cosine of the scattering angle for 0.5 MeV and 14 MeV; at the latter energy $\sqrt{\overline{\delta^2 \omega_1}}/\omega_1 \approx 0.15$.

Thus, for the correlation function $\rho_1 \, (E, E') \equiv \overline{\delta \omega_1(E) \, \delta \omega_i(E')}$ we take

$$
\rho_i(E,E') =
\begin{cases}
\overline{\delta^2 \omega_1 (E_{i-1})} \dfrac{(E_i - E)(E_i - E')}{(E_i - E_{i-1})^2} + \overline{\delta^2 \omega_1 (E_i)} \dfrac{(E - E_{i-1})(E' - E_{i-1})}{(E_i - E_{i-1})^2}, \\[4pt]
\qquad\qquad\qquad (E, E' \in [E_{i-1}, E_i]); \\[10pt]
\overline{\delta^2 \omega_1 (E_i)} \dfrac{(E - E_{i-1})(E_{i+1} - E')}{(E_i - E_{i-1})(E_{i+1} - E_i)}, \\[4pt]
\qquad\qquad\qquad (E \in [E_{i-1}, E_i], E' \in [E_{i+1}, E_i]); \\[10pt]
0, \qquad\qquad\qquad (E < E_{i-1}, E' > E_i)
\end{cases}
$$

where $\overline{\delta^2 \omega_1 (E_i)} = \delta_i^2 \cdot \omega_1^2 (E_i)$ and the values of the relative errors in δ_i at energies E_i are given by Table 2.

<u>Table 2</u>

Relative errors in the values for the mean cosine
of the angle of elastic scattering

i	E_i (MeV)	δ_i, %
0	0	0
1	0.5	50
2	2.5	30
3	14	15

5. <u>Cross-section for the reaction D(n,2n)</u>

Experimental data on the cross-section for the reaction D(n,2n) are presented in Fig. 5; the basic reference information about the corresponding

- 14 -

works is presented in Table 6. Most of the experimental data derive from
the direct measurement of σ_{2n} [N-1, N-2, N-3, N-4]. In estimating the energy
dependence of the cross-section in the high-energy region ($\sim$ 14 MeV) we also
used Refs [N-5] and [N-6], in which the angular distribution of the elastically
scattered neutrons was measured and an estimate made of the cross-section
for the reaction D(n,2n) as the difference $\sigma_t - \sigma_{el}$. In the same way, we
determined σ_{2n} from the data in Ref. [E-13] (see Table 5), the authors of
which measured the angular distribution of elastically scattered neutrons
over a wide range of angles (from 13.5° centre-of-mass*/ to 158° centre-
of-mass*/).

Figure 5 gives the results obtained by calculating the energy dependence
of σ_{2n} for deuterium from Refs [16] and [33]. The considerable difference
between the calculation results reflects the complexity of the structure
of the quantitative model of a n-d interaction.

Accordingly, in estimating $\sigma_{2n}(E)$ we relied exclusively on experimental
data.

The errors in the estimated cross-section for the reaction (n,2n) in
the region from the threshold to 15 MeV may be considered strongly correlated:

$$\delta \overline{\sigma_{2n}}(E) \cdot \delta\overline{\sigma_{2n}}(E') = \delta_{2n}^2 \cdot \overline{\sigma_{2n}}(E) \cdot \overline{\sigma_{2n}}(E') ;$$

the accuracy of the estimated cross-section $\delta_{2n} \approx 10\%$.

6. Energy-angular distributions of neutrons emitted
in the reaction D(n,2n)

Experimental information about the energy-angular spectra of neutrons
emitted in the reaction D(n,2n) is very scarce, so that the present estimate
of these spectra is based mainly on their theoretical description. Use
is made of the simplest model of this reaction – the breakdown of a compound
nucleus into two neutrons and a proton without allowance for any interaction
among the nucleons as they fly apart (the phase-space model).

According to this model, the angular distributions of the non-interacting
and stable particles formed as a result of the breakdown of a nucleus are
isotropic in the centre-of-mass system and the energy distribution of each
of the particles in the same system of co-ordinates has the form [1]

$$N(E_c,\mu_c)dE_c\,d\mu_c = Const \cdot \sqrt{E_c(E_c^{max} - E_c)} \cdot dE_c \cdot d\mu_c, (I)$$

*/ Translator's note – This is a guess; in the original there are only
abbreviations.

where E_c^{max} is the maximum energy which the particle under consideration can have in the centre-of-mass system.

In the laboratory system of co-ordinates, the energy-angular distribution of the neutrons has the same form:

$$N(E_L, \mu_L) = C(E') \cdot \sqrt{E_L [E_L^{max}(E_L', \mu_L) - E_L]} \ , \qquad (2)$$

where E_L' is the initial and E_L the final neutron energy in the laboratory system of co-ordinates and E_L^{max} is the maximum possible energy of a neutron escaping at an angle arccos μ_L.
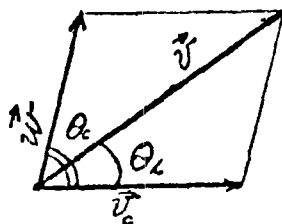
Fig. 6. Velocity diagram

$V, \theta_L; W, \theta_c$ — velocity of neutron after collision and angle of scattering in laboratory system of co-ordinates and centre-of-mass system respectively.

$(\mu_L = \text{Cos } \vartheta_L; \quad \mu_c = \text{Cos } \vartheta_c$

V_c — velocity of centre-of-mass.

For the energy of the neutron under consideration to be at its maximum, the other particles formed in the reaction — a neutron and a proton — must fly in the centre-of-mass system in the direction opposite to the direction of movement of the neutron under consideration. Hence, from the reaction kinematics point of view it is possible to regard these two particles as a single particle — an unbound deuteron. The deuteron binding energy expended in the reaction appears in the same way as the excitation energy of the nucleus in inelastic scattering. For inelastic scattering, $E_L^{max}(\mu_L)$ has the form (see formula (60) in Ref. [17][*])

$$E_L^{max}(\mu_L) = E' \frac{2\mu_L^2 + \frac{M^2}{m^2}(1 + \frac{M+m}{M} \cdot \frac{Q}{E'}) - 1 \pm 2\mu_L \sqrt{\mu_L^2 + \frac{M^2}{m^2}(1 + \frac{M+m}{M} \cdot \frac{Q}{E'}) - 1}}{(\frac{M}{m} + 1)^2} , \qquad (3)$$

---

[*] In formula (60), the first term in the numerator should be $2\mu_L^2$ and not $2\mu_L$.

where **M** is the deuteron mass,

m is the neutron mass,

Q is the reaction energy (Q = -2.225 MeV).

If $E' > E_{form}^{*/} = -Q \cdot M/(M-m)$, the minus sign in formula (3) must be discarded as μ_L may, in this case, assume any value from +1 to -1. Near the reaction threshold, for

$$3.34 \text{ MeV} = -Q(M+m)/M = E_{thr} \leq E' \leq E_{form} = 4.45 \text{ MeV}^{*/}$$

neutrons from the reaction (n,2n) in the laboratory system of co-ordinates are observed only at forward angles:

$$\mu_L < \mu_L^{min} = (M+m)\sqrt{-\frac{Q}{E'} \cdot \frac{M}{M+m} - \frac{M-m}{M+m}} \qquad (4)$$

In this range of angles one should consider two groups of neutrons - the spectrum of one of them is determined by formula (2), in which E_L^{max} is calculated according to formula (3) using a plus sign and the spectrum of the other one according to the same formula but with E_L^{max} calculated using a minus sign.

The constant C(E') in formula (2) is determined from the normalization condition:

for $E' > E_{form}$:
$$\int_{-1}^{+1} d\mu_L \int_0^{E_L^{max}(\mu_L)} N(E_L, \mu_L) d\mu_L = 1 \qquad (5)$$

for $E_{trans}^{**/} \leq E' \leq E_{form}$:
$$\int_{\mu_L^{min}}^1 d\mu_L \left\{ \int_0^{E_L^+(\mu_L)} N_+(E_L, \mu_L)dE_L + \int_0^{E_L^-(\mu_L)} N_-(E_L,\mu_L)dE_L \right\} = 1 \qquad (6)$$

---

*/ Translator's note - I have assumed that the two unexplained Russian subscripts denote "formation energy" and "threshold energy".

**/ Translator's note - I have assumed that the unexplained Russian subscript denotes "transition energy".

The following formulas are derived for $C(E')$ on the basis of these conditions:

$$C(E') = \frac{2 \cdot (M + m)^4}{\pi^2 \cdot E'^2 \cdot m^4 \left(a^2 + \frac{8}{3} a + \frac{8}{5} \right)}, \text{ for } E > E_{form} \qquad (7)$$

$$C(E') = \frac{2 \cdot (M + m)^4}{\pi^2 \cdot E'^2 \cdot m^4 \left[a^2 \left(1 - \mu_L^{min}\right) + \frac{8}{3} a \left(1 - \mu_L^{min 3}\right) + \frac{8}{5} \left(1 - \mu_L^{min 5}\right) \right]} \qquad (8)$$

$$\text{for } E_{thr} \leq E' \leq E_{form}.$$

Here μ_L^{min} is a function of E' determined according to formula (4) and

$$a(E') = \frac{M^2}{m^2} \left(1 - \frac{M + m}{M} \cdot \frac{Q}{E'} \right) - 1. \qquad (9)$$

Thus, the energy-angular distribution of neutrons from the reaction $(n,2n)$ is completely determined.

It should be noted that the breakdown model used above is an approximate one. In particular, it does not take into account the effect of direct interactions, which become appreciable at high incident neutron energies $(E' > 10 \text{ MeV})$ and escape angles close to $0°$ and $180°$. Under these conditions, the processes of nucleon interaction in the final state are so important that the reaction $D(n,2n)$ may be regarded qualitatively as $D(n,n')D^*$, $D(n,D^*)n$, $D(n,p)B$ or $D(n,B)H$, where D^* denotes an unbound (virtual) deuteron and B denotes a virtual bineutron. The direct nature of these reactions shows up in the fact that the angular distributions of the reaction products have sharp directionality forwards and, correspondingly, backwards. In the spectrum of the neutrons escaping at small angles there must be observed an excess of neutrons with energies close to the maximum owing to the reaction $D(n,n')D^*$ and half as much energy owing to the reactions $D(n,D^*)n$ and $D(n,B)H$. At angles close to $180°$, for $E \sim E_{max}$ a peak owing to the reaction $D(n,D^*)n$ is to be expected in the neutron spectrum and for $E \approx E_{max}/2$ a peak owing to the reaction $D(n,p)B$ is to be expected.

In the spectrum of the protons formed in the reaction $D(n,2n)$ and escaping at small angles, one should also observe maximum when $E \sim E_{max}$ (owing to the reaction $D(n,p)B$) and $E \sim E_{max}/2$ (owing to the reaction $D(n,D^*)n$).

Such maxima show up clearly in the experimental spectra of protons from the reaction $D(n,2n)p$ measured in Ref. [19] at a neutron energy of 14.4 MeV (see Figs 7a and 7b).

It should be noted that the cross-sections for the reactions involving the formation of a virtual bineutron and a virtual deuteron must, generally speaking, be different as the deuteron can form in both the singlet and the triplet state while the bineutron - because of the Pauli principle - can form only in the singlet state. The cross-sections for the reactions $D(n,D^*)n$ and $D(n,n')D^*$, and the reactions $D(n,B)p$ and $D(n,p)B$, may also be different: the first of each pair of reactions is a pick-up reaction while the second of each pair is like stripping or an exchange process $(D(n,n')D^*)$.

As there is very little information about the direct mechanisms of the reaction $D(n,2n)$, it is interesting to consider data concerning the influence of these mechanisms on the reactions $D(p,n)$ and $H(d,n)$.

The results of measurements of the spectra of neutrons excaping at an angle of $0°$ to a beam of 8.9 MeV protons striking a deuterium target are presented in Ref. [35]. The authors of Ref. [36] measured the spectrum of neutrons escaping in the forward direction from the reaction $H(d,n)$ for a deuteron energy of 18.6 MeV. This spectrum may also be regarded as the spectrum of neutrons escaping in the backward direction from the reaction $D(p,n)$ occurring through the action of 9.3 MeV protons.

V.V. Komarov and A.M. Popov [22] carried out a theoretical analysis of these data. The neutron spectra calculated by them are in excellent agreement with the experimental spectra. It was found that the peaks in the spectrum of neutrons escaping in the forward direction are due to a reaction of the type $D(p,n)He^2$ (near the maximum energy) and $D(p,D^*)H$ (in the intermediate energy region). The blurred peak in the spectrum of neutrons escaping in the forward direction is due almost entirely to a reaction of the type $D(p,He^2)n$; thus, the escape of an unbound deuteron in the backward direction is improbable. It was also found that the (p,n) interaction is almost entirely a singlet reaction.

The nature of the spectra of neutrons escaping in the backward direction from a $D(p,n)$ reaction is preserved even with lower proton energies. According to the data of Poppe et al. [20], who measured the spectra of neutrons escaping in the forward direction from the reaction $H(d,n)$, the influence

of the reaction $D(p,He^2)$ manifests itself already when $E_p \sim 5$ MeV. With lower proton energies, the neutron spectra are described within the error limits by breakdown spectra (see Fig. 8).

Let us now return to the estimate of the cross-sections for direct interactions in the reaction $D(n,2n)$. The angular distributions of neutrons produced by the reactions $D(n,D^*)$ (peak at intermediate energies of protons escaping in the forward direction) and $D(n,p)B$ (peak at maximum energy) are presented in Fig. 9. The data were obtained by integrating those parts of the proton spectra from Ref. [19] which lie above the breakdown spectrum. The amplitude of the breakdown spectrum was estimated from the distributions at $30°$ and $45°$, where the contribution of direct processes is small ($30°$) or non-existent ($45°$). When the total cross-section for the reaction $D(n,2n)$ at 14.4 MeV is, according to the estimate made above, 170 mbarn, the cross-sections for the reactions $D(n,D^*)n$ and $D(n,p)B$ are 3.6 mbarn and 2.2 mbarn respectively.

In accordance with the results of the analysis of direct interactions in the reaction $D(p,n)$, the cross-section for the reaction $D(n,n')D^*$ is taken to be zero and the cross-section for the reaction $D(n,B)H$ is taken, on the assumption that

$$\frac{D(n,B)H}{D(n,D^*)n} = \frac{D(p,He^2)n}{D(p,D^*)p} \approx \frac{1}{1.5},$$

to be 2.4 mbarn. Thus, the value of the total cross-section for the reaction $D(n,2n)$ at 14.4 MeV due to a direct interaction is ~ 8.2 mbarn. As regards the energy dependence of the direct process cross-sections, on the basis of the data of Poppe et al. [20], which indicate that direct processes start to manifest themselves when the reaction threshold is exceeded by about 1.5 MeV, we assumed a linear growth of the cross-sections with energy, beginning at the inverse*/ threshold of the reaction $D(n,2n)$ (at 4.45 MeV).

The angular distributions of the products of the reaction $D(n,B)H$ were taken by us to be the same as those of the products of the reaction $D(n,p)B$;

---

*/ Translator's note - Or should this be "reverse"?

that is in accordance with the data on the angular distribution of the products of the reaction $D(p,He^2)n$ [20]. The angular distributions of the products of all direct reactions are approximated by triangles in the recommended data (see Fig. 9).

The energy distributions of neutrons formed in direct processes are taken to be as follows:

    -   for the reaction $D(n,D^*)n$,

$$f(E,\mu) = f_{\mathcal{D}}*(\mu) \cdot \delta\left[E - E_\lambda^{max}(\mu)/2\right] + f_{\mathcal{D}}*(-\mu) \cdot \delta\left[E - E_\lambda^{max}(-\mu)\right]; \quad (9)$$

    -   for the reaction $D(n,B)H$,

$$f(E,\mu) = f_B(\mu) \cdot \delta\left[E - E_\lambda^{max}(\mu)/2\right]; \quad (10)$$

    -   for the reaction $D(n,p)B$,

$$f(E,\mu) = f_B(\mu) \cdot \delta\left[E - E_\lambda^{max}(-\mu)/2\right]; \quad (11)$$

where E_L^{max} is determined in accordance with formula (3) or through the cosine of the scattering angle in the centre-of-mass system (see formula (46) in Ref. [17]):

$$E_\lambda^{max}(\mu c) = E'\left[1 - \frac{2Mm}{(M+m)^2}\left(1 - \frac{M+m}{2m} \cdot \frac{Q}{E'} - \mu_c\sqrt{1 + \frac{M+m}{m} \cdot \frac{Q}{E'}}\right)\right]; (12)$$

7. Group constants

Annex 1 contains 26 group constants of deuterium obtained on the basis of estimated cross-sections, spectra and angular distributions of neutrons. In addition to the groups taken from Ref. [23] there are a (-1) and a zero group (see Tables 7-9). These groups have been introduced for thermonuclear reactor calculation purposes. The intragroup spectra taken in averaging are the same as in Ref. [23]: in groups (-1)-3 the fission spectrum and in the lower groups the Fermi spectrum.

The probability of intergroup neutron transitions as a result of the reaction $(n, 2n)$ and their angular momenta (W_i^{ℓ}) were calculated with the help of energy distribution function (3) described in Section 6 (using the MATRA program written for this case) as follows:

- for $E' > E_{form}$,

$$W_i^{\ell} = \frac{\int_{E_i}^{E_{i-1}} \sigma_{2n}(E') \cdot \mathcal{Y}(E') \cdot dE' \int_{-1}^{+1} d\mu_{\lambda} \int_{E_j}^{E_{j-1}} N(E_{\lambda}, \mu_{\lambda}) \cdot P_{\ell}(\mu_{\lambda}) \cdot dE_{\lambda}}{\int_{E_i}^{E_{i-1}} \sigma_{2n}(E') \cdot \mathcal{Y}(E') \cdot dE'} \; ;$$

- for $E_{trans} \leq E' \leq E_{form}$,

$$W_i^{\ell} = \int_{E_i}^{E_{i-1}} \sigma_{2n}(E') \cdot \mathcal{Y}(E') \, dE' \left\{ \int_{\mu_{\lambda}^{min}}^{1} d\mu_{\lambda} \int_{E_j}^{\tilde{E}_{j-1}} \left[N_+(E_{\lambda}, \mu_{\lambda}) + \right. \right.$$

$$\left. \left. + N_-(E_{\lambda}, \mu_{\lambda}) \right] \cdot P_{\ell}(\mu_{\lambda}) \, d\mu_{\lambda} \right\} \Big/ \int_{E_i}^{E_{i-1}} \sigma_{2n}(E') \cdot \mathcal{Y}(E') \, dE' \; .$$

Here, E_i and E_{i-1} are the energy boundaries of group i, from which occurs the impingement of neutrons on the lower groups j as a result of the reaction $D(n, 2n)$, E_j and $\tilde{E}_{j-1}$ are the energy boundaries of group j (if $E_L^{max} \leq E_{j-1}$, then $\tilde{E}_{j-1} = E_L^{max}$), $\mathcal{Y}(E')$ is the fission neutron spectrum for the energies under consideration ($E' > 2.5$ MeV) and P_{ℓ} is a Legendre polynomial of the order ℓ.

The group constants of deuterium are presented in Table 7. In contrast to Ref. [23], the curve with values of the mean-logarithmic energy loss ξ is excluded here, for the age approximation - in which this quantity is used - is not generally employed in the case of deuterium.

Table 8 shows the group parameters of elastic scattering anisotropy; they differ somewhat from the values published earlier [17] owing to the appearance of new data (see Section 4).

Lastly, we give in Table 9 the matrices of the moments of the cross-section for the reaction $D(n,2n)$. In these matrices, the presence of direct processes is taken into account in accordance with Section 6. When using the Table 9 data, one should remember that they relate to one neutron resulting from the reaction $D(n,2n)$.

8. Presentation of evaluated data in the SOCRATOR format

The contents of the file of evaluated neutron data for deuterium in the SOCRATOR format [24] is presented in tabular form in Annex 2.

The library number of the file is 2003. Hence, the identifying nuclear number is 200301002.

The file has nine sections.

Section 0 - Heading.

Section 1 - $\underline{\text{NTR}}^{*/}$ = 01001 - Total cross-section data. As for the other cross-sections, a point-by-point description is used for the energy dependence of the cross-section (NTP = 111) with interpolation between the points on a linear-linear scale (INT = 111000000). The number of points at which the cross-section is specified is 86.

Section 2 - NTR = 01102 - Radiative capture cross-section; specified at the same energy points as the total cross-section.

Section 3 - NTR = 01002 - Elastic scattering cross-section; specified at the same energy points as the total cross-section.

Section 4 - NTR = 02002 - Angular distributions of elastically scattered neutrons in the laboratory system of co-ordinates; specified point by point in the ω representation at the same points as the elastic scattering cross-section (HTP = 211). Five expansion coefficients are presented (up to ω_5 inclusive). This number of expansion coefficients is sufficient for describing all observed angular distributions in the energy region below 15 MeV.

$^*/$ Translator's note - This and other abbreviations are not explained in the original.

Section 5 - NTR = 03002 - Energy spectrum of elastically scattered
neutrons; specified by law No. 10 [24].

Section 6 - NTR = 01016 - Cross-section for the reaction $(n, 2n)$;
specified in two energy ranges. In the energy region from 10^{-4} eV to
3.339 MeV the cross-section is zero. Above 3.339 MeV up to 15 MeV the cross-
section is specified at 25 energy points (the cross-sections for the other
reactions are presented at the same energies).

Section 7 - NTR = 2016 - Angular distributions of neutrons from the
reaction $(n, 2n)$; specified in two energy ranges. In the first range, from
the forward threshold (3.339 MeV) to 4.45 MeV (inverse[*]/ threshold), data
are presented for both neutrons from the reaction $(n, 2n)$. The angular
distribution of these neutrons is taken to be isotropic in the centre-of-mass
system (NTP = 201). In the range from 4.45 MeV to 15 MeV, where direct
processes are important, the data are presented separately for the "first"
and the "second" neutrons emitted in the reaction $(n, 2n)$. For each of these
groups of neutrons, the angular distributions are described by a superposition
of four angular distributions specified in the centre-of-mass system in the
μ representation (NTP = 121).

The probability of the first angular distribution is equal to the
probability of the breakdown mechanism; the corresponding angular distri-
bution is isotropic.

The second angular distribution relates to neutrons emitted as a
result of the process $D(n, B)H$; this distribution falls linearly to zero
as μ_C decreases from 1 to 0.94.

The third angular distribution describes neutrons formed as a result of
the reaction $D(n, p)B$; this distribution falls linearly to zero as μ_C changes
from -1 to -0.94.

The fourth angular distribution describes neutrons formed as a result
of the reaction $D(n, D^*)n$. It is accepted that the "first" neutrons escape
in the forward direction and their angular distribution falls to zero for
$\mu_C = 0.955$ and that the "second" neutrons escape in the backward direction
and their angular distribution is symmetric with the angular distribution
of the first neutrons. It is this process which gives rise to the difference
between the angular distributions of the "first" and the "second" neutrons.

---

[*]/ Translator's note - Or should this be "reverse"?

The probabilities of the angular distributions are specified at two energy points at the edges of the energy range, between which linear interpolation is envisaged. The probabilities of direct processes at the lower energy boundary of the range are zero.

Section 8 - NTR = 3016 - Energy distributions of neutrons from the reaction (n,2n); specified in the same energy ranges as the angular distributions.

In the first range, the energy distribution is due entirely to the breakdown mechanism. Of the laws envisaged by the format [24], the only one which enables this distribution to be described is law No. 8, for which it is necessary to specify an arbitrary function of the initial and final energy of the neutron. As a rule it is best not to use this law, because it is cumbersome and because of the inevitable distortion of the spectra during interpolation with normalization.

In our case, the use of this law is especially undesirable also because one thereby loses the chance of taking into account the correlations between the spectrum and the escape angle of neutrons from the reaction (n,2n), which are very strong. For these reasons we decided to introduce a new law into the format - law No. 13 (NTP = 113), which describes the energy-angular distributions of neutrons from the breakdown reaction. This law can also be used for specifying the spectra of neutrons for the reactions $T(n,2n)$, $He^3(n,2n)$, etc.

In the second energy range, the data are presented - as in the case of angular distributions - for two groups of neutrons from the reaction (n,2n): "first" and "second" neutrons. For each of these groups, the energy distributions are described by a superposition of four laws (NTP = 151) relating to neutrons from the breakdown process and the processes $D(n,B)H$, $D(n,p)B$ and $D(n,D^*)n$. The probabilities of these processes are naturally the same as those specified in Section 7. The energy distributions of the breakdown neutrons are specified, as in the first range, by law No. 13. As regards the energy distributions of neutrons formed as a result of direct interactions, there were two possibilities - either to describe them by δ-functions independent of the escape angle of the neutrons (law No. 2, NTP = 102) or to modify law No. 10 (NTP = 110) describing the inelastic scattering spectra (with allowance for their dependence on the escape angle).

The required modification is a simple one: it is necessary only to introduce a coefficient m indicating by how many times the mass of the escaping particle (bineutron or unbound deuteron) is greater than the neutron mass (the use of which is envisaged by the standard form of law No. 10 a priori). The energy calculated using the true mass of the escaping particle must then be divided between the component nucleons in proportion to their masses - i.e. the energy of the escaping neutron is $\frac{1}{m}$ times the energy of a particle with a mass equal to m neutron masses. It is not difficult to take this modification into account in the program for processing the data presented by law No. 10 as, in this case, the format allows the coefficient m to be written in the reserve position (the second position of the card of the corresponding NTP - see Ref. [24]).

Accordingly, we thought it best to take this modification of law No. 10 and to use it for specifying the energy distributions of neutrons emitted in direct processes.

A description of the changes in and additions to the formats for presenting data on the energy distributions of the secondary particles about which we spoke above is contained in Ref. [34].

REFERENCES

1. Horsley A. Nuclear Data, A4, 1968, p. 321.
   Horsley A. LA-3271, 1967.
2. Leonard B.R., Jr., Nuclear Technology, 1972, v.15,c.49.
3. Stehn J.R., Goldberg M.D., Magurno B.A., Wiener -
   Chasman R., BNL-325, 2 Edition, Supplement 2, 1964.
[4] HARMS, E., LEROZE, L., private communication, presented in [C-16]*/.
5. Merritt J.S., Taylor J.C.V., Boyd A.W. Nucl.Sci.Eng.,
   1968, v.34, p.195.
6. Merritt J.S., Taylor J.G.V., Boyd A.W. Nucl.Sci.Eng.,
   1967, v.28, p.286.
7. Jurney E.T., Motz H.T., AML-6797, 1963, p. 236.
8. Kaplan L., Ringo G.R., Wilzbach K.E. Phys.Rev., 1952,
   v. 87, p. 785.
9. Bösch R., Lang J., Müller R., Wölfli W. Phys. Lett.,
   1964, v.8, p.120.

---

*/ Translator's note - The meaning of "[C-16]" is not clear.

10. Kosiek R., Müller D., Pfeiffer R. Phys. Lett., 1966, v. 21, p. 199.

11. Gunn J.C., Irving J., Phil. Mag., 1951, v. 42, p.1353.

12. Cerineo M., Ilakovas K., Slaus I., Tomas P., Phys. Rev., 1961, v. 124, p. 1947.

13. Tudoric-Ghemo J., Tomas P., Slaus I. Miljanic D., Antwerpen., 12-13 July, 1965, p. 136.

[14] NIKOLAEV, M.N., BAZAZYANTS, N.O., Anisotropy of the elastic scattering of neutrons (in Russian), Atomizdat, Moscow, 1972.

[15] BAZAZYANTS, N.O., ZABRODSKAYA, A.S., LARINA, A.F., NIKOLAEV, M.N., in "Jadernye konstanty" ("Nuclear constants"), issue 8, part 1, page 61, TsNIIATOMINFORM, Moscow, 1972.

[16] FRANK, R.M., GAMMEL, J.L., Phys. Rev., 1954, v.93, p. 463.

[17] BAZAZYANTS, N.O., ZABRODSKAYA, A.S., NIKOLAEV, M.N., in "Jadernye konstanty" ("Nuclear constants"), issue 8, part 2, page 3, TsNIIATOMINFORM, Moscow, 1972.

18. Stewart L., LA 3270, 1965.

19. Ilakovac K., Kuo L.G., Petravic M., Slaus I., Tomas P., Phys. Rev. Lett., 1961, v.6, p.356. Nucl.Phys., 1963, v.43, p.254.

20. Poppe C.H., Holbrow C.H., Borchers R.R. Phys.Rev., 1963, v. 129, p. 733.

21. Delves L.M. Nucl.Phys., 1961, v.26, p.136.

[22] KOMAROV, V.V., POPOVA, A.M., Zh. Ehksp. Teor. Fiz. 38 (1960) 1559.

[23] ABAGYAN, L.P., BAZAZYANTS, N.O., BONDARENKO, I.I., NIKOLAEV, M.N., "Group constants for nuclear reactor calculations" (in Russian), Atomizdat, Moscow, 1964.

[24] KOLESOV, V.E., NIKOLAEV, M.N., in "Jadernye konstanty" ("Nuclear constants"), issue 8, part 4, page 3, TsNIIATOMINFORM, Moscow, 1972.

25. Holden N.E., Walker F.W. The Chart of the Nuclides, Knolls atomic power lab, 11-th edition revised to april 1972, printed in USA.

26. Mattauch J.H.E., Thiele W., Wapstra A.H. Nucl.Phys., 1965, v.67, p.1.

27. Ozer O., Garber D."ENDF/B Summary Documentation", BNL 17541 (ENDF-201), May 1973.

28. Brolley J.Jr., Putnam T.M., Rosen L., Stewart L.,
Phys. Rev., 1960, v.117, p.1307.

29. Allred J.C., Armstrong A.H., Bondelid R.O., Rosen L.
Phys.Rev., 1952, v. 88, p.433.

30. Van Oers W.T,H., Brookman K.W.Jr., Nucl. Phys., 1960,
v. 21, p. 189.

[31] VAN OERS, W.T.H., BROCKMAN, K.W. Jr., private communication, contained
in Ref. [1].

[32] KIKUCHI, S., SANADA, J., SUWA, S., HAYASHI, I., NISIMURA, K.,
FUKINAGA, K., J.Phys.Soc., Japan, 1960, v.15, p. 9.

[33] SLOAN, J.H., Nucl. Phys., 1971, v. A168, p. 211.

[34] NIKOLAEV, M.N., "Changes in the format of the SOCRATOR library of
evaluated nuclear data" (in Russian), in "Jadernye konstanty" ("Nuclear
constants"), issue 16, page 35, Atomizdat, 1974.

[35] NAKADA, M.P., ANDERSON, J.D., GARDNER, C.C., McCLURE, J., WONG, C.,
Phys. Rev., 1958, v. 110, p. 594.

[36] VLASOV, N.A., KALININ, S.P., RYBAKOV, B.V., SIDOROV, V.A.,
proceedings of international conference on nuclear physics, Paris, 1958.

Table 3
(1)
Reference and bibliographic data on experimental work
relating to the total cross-section of deuterium

Worth	Author(s)	Laboratory	Published in	Year of publ.	Element studied
P - I	Nuckolls R.G., Bailey C.L., Bennett W.E., Bergstralh Th., Richards H.T.	Illinois Institute of Technology U.S.N.R. University of Wisconsin University of Minnesota	Phys.Rev., 70, 805	1946	D, C
P - 2	Bretscher E., Martin E.B.	A.E.R.E. Harwell Londonderry Laboratories for Radiochemistry	Helv. Phys., Acta, A23, 15	1950	D C O
P - 3	Goodman L.S.	ANL	Phys. Rev., 88, 686	1952	H, D, Be, C, O, Mg, Al, Ti, V, Cr, Fe, Ni, Cu, Zn, Zr, Mo, Sn, Sb, W, Pt, Pb
P - 4	Poss H.L., Salant E.O., Snow G.A., Yuan L.C.L.		Phys. Rev., 87, 11	1952	
P - 5	Zimmerman R.L., Cooper D.I., Frisch D.H.	ORL and AEC	Phys. Rev., 90, 339 A	1953	D
P - 6	Adair R.K., Okazaki A., Walt M.	University of Wisconsin	Phys. Rev., 89, 1165	1953	D
P - 7	Tunnicliffe P.R.	AERE Harwell	Phys. Rev., 89, 1247	1953	D
P - 8	Cook C.P., Bonner T.W., Allen W.D., Ferguson A.T.G., Roberts J.	Rice Institute AERE Harwell	Phys. Rev., 94, 651 Proc. Phys., Soc., 68A, 650	1955	H, D, Li, Be, ^{10}B, ^{11}B,C,C, Mg, Al, S D
P - 9	Seagrave J.D., Henkel R.L.	LASL	Phys. Rev., 98, 666	1955	D
P -10	Bratenahl A., Peterson J.M., Stoering J.P.	University of California	Phys. Rev., 110, 927	1958	H,D,^{6}Li, ^{7}Li,Be, C, F, Mg,Al, Ti,Cr,Fe,Ni,Cu,Zn, Ga,Ge,Zr,Mo,Pd, Ag, Cd, In,Sn,Sb,Te,W,Pt,Au,Tl, Pb, Bi
P -II	Willard H.B., Bair J.K., Jones C.M.	ORNL	Phys. Lett., 9, 339	1964	D
P -I2	Glasgow D.W., Foster D.G.Jr.	Battelle Memorial Institute, Washington	Phys. Rev., 157, 764	1967	D
P -I3	Davis J.C., Barschall H.H.	University of Wisconsin	Phys. Rev., C3, 1798	1971	D
P -I4	Clement J.M., Stoler P., Golding C.A., Fairchild R.W.	Rensselaer Polytechnic Institute Troy, New York	Nucl. Phys., A183, 51	1972	H, D
P -I5	Stoler P., Kaushal N.N., Green F.; Stoler P., Kaushal N.N., Green P., Harms E., Laroze L.	Rensselaer Polytechnic Institute Fairfield University Connecticut.	USNDC-9 EANDC(US)- 176 " ",155. Phys. Rev. Lett., 29, 1745	1972 1972	D

Table 3
(2)

Reference and bibliographic data on experimental work
relating to the total cross-section of deuterium
(contd.)

Neutron source	Energy resolution (MeV)	Neutron energy (MeV)	Detector	Method	Comments
$^7Li(p,n)$ $^{12}C(d,n)$ $^2H(d,r)$	0,1 at 1,0 MeV	0,37 → 0,97 1,0 → 2,0 2,0 → 6,0	Ionization chambers of different dimensions	Transmission	σ obtained by comparing the transmission of heavy and ordinary water. No corrections were introduced for multiple scattering owing to their smallness
0.25-0.65 MeV from the reaction [omission in original] 2.0-4.0 MeV from the reaction [omission in original]		0,22 → 4,05 0,26 → 3,8 0,22 → 4,05 0,26 → 2,35	Hydrogen-filled proportional counter ($\emptyset$ 2.5 cm)	Transmission	No corrections were introduced for the finite dimensions of the sample and counter as they are small with the geometry used
T(d,n)		14	Anthracene crystal	Transmission	
$^7Li(p,n)$	0,1 → 0,55		Recoil proton proportional counter	Transmission	
$^7Li(p,n)$ T(p,n)		0,262 → 0,872 1,178 → 2,962	Cylindrical pulsed ionization chamber	Transmission	σ obtained by comparing the transmission of heavy and ordinary water
$^7Li(p,n)$		0,1 → 1,0	Proportional counter containing deuterium gas	Direct measurements of energy distribution of recoil deuterons	Absolute value of neutron flux determined with hydrogen filled counter
T(d,n)	0,020 → 0,040	14,1 → 18,0	Threshold anthracene scintillator	Transmission	
T(p,n)	0,012 0,1	0,10 0,146 0,20	Proportional counter containing deuterium gas	Measurement of energy distribution of recoil deuterons	Overall statistical accuracy ± 3%
T(p,n) D(d,n) T(d,n)	0,040 → 0,010 0,062 → 0,017 0,200 → 0,030	0,267 → 4,002 4,390 → 8,126 14,35 → 21,35	Stilbene scintillator	Transmission	Cross-section measurement accuracy ~ 2% Sample - gaseous deuterium
D(d,n)	0,17 7 MeV 0,07 14,0	7,0 → 14,0	Plastic scintillator	Transmission	Time-of-flight method. Cross-section measurement accuracy ± 1-2%
D(d,n)	0,02 3	2,8 → 3,6	Stilbene scintillator	Transmission	Relative probable accuracy of data ~ 4%
$^3Li(d,n)$	0,045 → 0,077	2,25 → 15,0	Liquid organic scintillator ~ 213	Transmission	Time-of-flight method. Accuracy of determination of data 5.7 ± 1.0%. σ_t measured for 241 different energies. Sample - deuterium hydrocarbonate
T(p,n) D(d,n) T(d,n)	0,015 → 0,020 0,06 0,02 → 0,05	1,5 → 6,7 6,7 → 15 2,0 → 26	Cylindrical stilbene scintillator	Transmission	Accuracy of cross-section determination 1-2% Sample - deuterium hydrocarbonate
Continuous spectrum of neutrons from linear electron accelerator		0,5 → 30	Seven separate recoil proton liquid scintillators	Transmission	Time-of-flight method. Flight distance 250 m. Sample containing 99.5% deuterium or 99.9% hydrogen in the gaseous state
Continuous spectrum of neutrons from linear electron accelerator		(0,001)→1,0	NaI detector in $^{10}B_4C$	Transmission	Time-of-flight method. Flight distance 33 m. Two gaseous samples with different pressures were used.

Table 4

Reference and bibliographic data on the cross-section for slow neutron scattering on deuterium

Work	Author(s)	Laboratory	Where and when published	What was measured	Method	Result
T-1	Fermi E., Marshall L.	A.N.L. / I. for Nucl. St.	Phys. Rev., 75, 578 (1949)	1) $\sigma(D_2)$ 2) $\sigma(D)$	Transmission. Detector - long counter with BF_3. In (1) thermal neutrons; in (2) E_n ~ Ag and In resonances	$\sigma(D_2) = 21.3 \pm 0.2$ barn, Ortho- and para-deuterium not separated. $\sigma(D) = 4\pi(2a_2^2/3 + a_2^2/3) = 3 \pm 0.06$ barn $\delta = (a_4 - a_2)^2/(2a_4^2 + a_2^2) = 0.04 \pm 0.1$ (from $\sigma(D_2)/\sigma(D)$).
T-2	Shull C.G., Wollan E.O.	ORNL	Phys. Rev., 81, 527 (1951)	1) σ_{coh} 2) σ_t 3) a_{coh}	Transmission. In (1) and (2) E_n ~ thermal. a_{coh} determined by diffraction spectroscopy method. Sample - crystalline powder.	$\sigma_{coh}(D)=4\pi(a_4+a_2/2)^2 =5.2\pm0.4$ barn $\sigma_t(D)=\frac{(A+1)^2}{A^2}\sigma_{free}=\frac{9}{4}\cdot 4\pi(a_4^2+a_2^2/2)=7.4\pm0.5$ barn $a_{coh}(D)=(a_4+a_2/2) = 6.4\pm0.2$
T-3	Hurst D.G., Alcock N.Z.		Can. J.P., 29, 36 (1951)	1) Intensity of neutrons scattered at different angles. 2) Total scattering cross-section.	In (1) neutron spectrometer (E_n ~ 0.072 eV). Deuterium in gaseous state at temp of liquid helium. In (2) transmission method.	$a_2/a_4 =0.12\pm0.04$, hence for $\sigma(D)= 3.14\pm0.06$ barn $a_2 = 0.7\pm0.3F$ and $a_4=6.38\pm0.06F$ $\sigma(D)=4\pi(2a_4^2/3+a_2^2/3)=3.4\pm0.4$ barn
T-4	Nikitin, S.Ya. Smolyansky, V.M. Kolganov, V.Z. Lebedev, A.V. Lomkatsi, G.S.	Inst. Theor. and Experim. Phys.	1st Geneva Conf., Vol. II, p. 99 (1955)	Cross-section for neutron scattering on ortho- and paradeuterium	Transmission. Neutrons filtered by beryllium. $E_n^{eff} = 0.0047$ eV. Sample in gaseous state at temp. of liquid hydrogen.	$\sigma_{ortho} = 8.33(2a_4 + a_2)^2 + 10.42(a_4 - a_2)^2 = 15.95 \pm 0.03$ barn. $\sigma_{para} = 8.33(2a_4 + a_2)^2 + 5.97(a_4 - a_2)^2 = 14.63 \pm 0.1$ barn. hence $a_2 = 0.57 \pm 0.14$ F, $a_4 = 6.47 + 0.14$ F
T-5	Gissler v.W.	Techn. Univ. München	Z. Krist, 118, 149 (1963)	D_2O transmission at t = 4° and 77° K	$E_n < 0.001$ eV	$\sigma_{incoh} = 2\pi(a_4-a_2)^2 = 2.25 \pm 0.04$ barn
T-6	Koester L., Ungerer H.	Techn. Univ. München	Z.P., 219, 300 (1969)	$a_{coh}(D_2O)$	Neutron reflection through small angles from a mixture of crystalline powder and a liquid.	$a_{coh} = 6.70 \pm 0.05$ F. Result obtained from $a_{coh}(D_2O) = 19.20 \pm 0.08$ F measured in the present work and $a_{coh}(O) = 5.8 \pm 0.05$ F taken from the work of Donaldson et al. (Phys. Rev. 138, (1965) B1116.
T-7	Bartolini W., Donaldson R.E., Groves D.J.	Univ. of California	Phys. Rev., 174, 313 (1968)	$a_{coh}(D)$ in relation to mercury and dimethyl naphthalene	Reflection from liquid glass.	$a_{coh}(D) = 6.21 \pm 0.04$ F (average of four measurements).
T-8	Ivanenko, A.I. Lushchakov, V.1. Taran, Yu.V. Shapiro, F.L.	Joint Inst. Nucl. Research	Yad. Fiz. 10 (1969) 47	Transmission of target containing polarized D, N, La nuclei	$E_n = 0.01 \div 40$ eV	Analysis of experim. data confirmed earlier conclusion that quartet length of neutron scattering on D greater than doublet length.
T-9	Dilg W., Koester L., Nistler W.	Techn. Univ. München	Phys. Lett., 36B, 208 (1971)	$a_{coh}(D_2O)$; $\sigma_{free}(O)$; $\sigma_{free}(D)$	Reflection from glass using a neutron gravitational refractometer. $E_n = 130$ eV. σ_{free} measured by transmission method.	From $a_{coh}(D_2O) = 19.148 \pm 0.015$ F, $\sigma_{free}(D) = 3.39 \pm 0.012$ barn and $\sigma_{free}(O) = 3.721 \pm 0.007$ barn one obtains $a_{coh}(O) = 5.804 \pm 0.007$ F, whence $a_{coh}(D) = 6.672 \pm 0.007$ F. From $\sigma_{free}(D)$ and $a_{coh}(D)$ it is found that $a_2(D) = 0.65 \pm 0.04$ F; $a_4(D) = 6.35 \pm 0.021$ F and $\sigma_{inc}(D) = 2.04 \pm 0.037$.

Table 5

Reference and bibliographic data on experimental work relating to the angular distribution of elastically scattered neutrons for deuterium

Work	Author(s)	Labora-tory	Where and when published	Measured distri-bution	Neutron source	Neutron energy E_n (MeV)	ΔE_n (MeV)	Detector	Investigated range, ϑ^o or $\cos \vartheta$	Comments
E-I	Wantuch E	BNL	Phys. Rev. 84.169 (1951)	Recoil neutrons from solid and gaseous target	D(d, n)	4,5 5,5	0,I	Proport. counter telescope, based on coincidences	80 ÷ 180 } centre 70 ÷ 180 } of mass	σ (4,5)=1,8±0,2 barn σ (5,5)=1,5±0,2 barn
E-2	Adair R.K., Okazaki A., Walt M.	Univ. of Wisconsin	Phys. Rev. 89.1163 (1953)	Recoil neutron	Li (p, n) T (p, n)	0,22;0,5 0,75;1,0; 1,5;2,0; 2,5.	0,25	Proport. counter for recoil nuclei with deuterium	~ 0,35 ÷ −0,75 centre of mass	Normalized to σ_t
E-3	Allen W.D., Ferguson A.T.G. Roberts J.	Harwell	Pr. P. Soc., A68,650 (1955)	Recoil deuterium and hydrogen nuclei	T (p, n)	0,I;0,2	0,012	Proport. counter for recoil nuclei with hydrogen and deuterium	~0,8 ÷ −0,75 centre of mass	Normalized to σ(H). Total statistical accuracy <3%.
E-4	Seagrave J.D. Granberg L.	LASL	Phys. Rev., IC5,1816 (1957)	Scattered neutrons, by time-of-flight method	T(p, n)	2,45 3,27	0,05	Scintill. counter	0,909 ÷ −0,965 }centre 0,855 ÷ −0,965 } of mass	Normalized to σ(H), $\Delta \vartheta$ = 3° centre of mass
E-5	Brüllmann M., Gerber H.J., Meier D., Scherrer P.	Phys. Inst. ETH, Zürich	HPA,32, 5II,(1959)	Recoil neutrons and scattered neutrons	D(d, n)	3,27	—	Scintill. counter for recoil nuclei with C_6D_6	53 ÷ I6I centre of mass	Plastic scintillator used for recording neutrons.
E-6	Elwyn A.J., Lane R.O., Langsdorf A.	ANL	Phys. Rev., 128,779 (1962)	Scattered neutrons	Li (p, n)	0,5;I,0; I,95	—	Proport. counter with BF_3 in modifier	22 ÷ I50 lab.	Normalized to σ(C), $\Delta \vartheta$ = 3-5° lab.
E-7	Blanc D., Cambou F., Vedrenne G.	Saclay	J. P. Colloque., I,71 (1966)	Recoil nuclei		3,22	0,06	Scintill. counter for recoil nuclei with C_6D_6	0,65 ÷ 0,96 centre of mass	
E-8	Bonner B.E., Paul S.B., Phillips G.C.	Rice University	N.P., A128.183 (1969)	Recoil deuterons; scattered neutrons, by time-of-flight method	D(d, n)	5,64 7,0I 9,04	—	Scintill. counter for recoil nuclei with C_6H_6 and C_6D_6	0,653 ÷ −0,826 }centre 0,620 ÷ −0,858 } of 0,760 ÷ −0,926 }mass	Normalized to σ(H). Plastic scintillator used for recording neutrons.
E-9	Seagrave J.D., Hopkins J.C., Dixon D.R., Keaton P.W. jr., Kerr E.C., Niller A., Sherman R.H., Walter R.C.	LASL	A.P., 74,250 (1972)	Scattered neutrons, by time-of-flight method	D(d, n)	5,55;7,0; 8,0; 9,0 18,55; 20,5; 23,0	—	Large liquid scintillator	0,695 ÷ −0,826 }centre 0,695 ÷ −0,912 } of 0,695 ÷ −0,871 }mass 0,695 ÷ −0,912 }	Normalized to σ(H). Accuracy of differential cross-section measure-ments ~ 7%.

Table 5

Reference and bibliographic data on experimental work relating to the angular distribution of elastically scattered neutrons for deuterium

Work	Author(s)	Laboratory	Where and when published	Measured distribution	Neutron source	Neutron energy E_n (MeV)	ΔE_n (MeV)	Detector	Investigated range, ϑ^o or $\cos \vartheta$	Comments
y-I0		L A S L	Phys. Rev. 91, 90 (1953)	Recoil deuterons	$T(d,n)$	14,1	0,10	Photonuclear emulsion	46 ÷ 176 centre of mass	Statistical accuracy 3.4-12%. $\Delta\vartheta$ = 5-10° centre of mass
y-II	Seagrave J.D.	L A S L	Phys. Rev. 97, 757 (1955)	Recoil deuterium and hydrogen nuclei	$T(d,n)$	14,1	0,05	Two proport. counters and one with NaI crystal	70 ÷ 174 centre of mass	Triple coincidence scheme. σ(14.1) = 0.61 ± 0.03 barn. Statistical accuracy 1.5-10%, $\Delta\vartheta$ = 4-7° centre of mass
y-I2	Shirato S., Kaori N.	St. Paul's University, Tokyo	N.P. A120, 387 (1968)	Recoil deuterons	$T(d,n)$	14,1	0,15	Telescope of three similar proport. counters with Si(Li)	80 ÷ 172 centre of mass	$\bar{\sigma}$ (14,1)=0,598 ± ±0,021 barn; $\Delta\theta$ = 2,32° centre of mass
y-I3	Berick A.C., Riddle R.A.J., York		Phys. Rev. 174, 1105 (1968)	Recoil deuterons; scattered neutrons by time-of-flight method		14,3	0,20	Plastic scintillator	13,5 ÷ 158 centre of mass	Normalized to σ(n,p) = 0.689 ± 0.005 barn. $\Delta\vartheta$ = 1.8° lab., $\Delta\vartheta$ = 1.2°-2.7° centre of mass. σ(14.3) = 0.648 ± 0.063 barn.

Table 6

Reference and bibliographic data on experimental work relating to the cross-section for the reaction (n, 2n) on deuterium

Work	Author(s)	Laboratory	Where and when published	Neutron source	Energy E (MeV)	E (MeV)	Detector	Method	Comments
N-I	Ashley V.J., Carlon A.C., Newkirk L.L., Taylor C.J.	University of California	Phys. Rev., III, 616 (1958)	$T(d,n)$	14,1	—	Large liquid scintillator with Cd; (n,2n) target located at centre of detector	Counting of double pulses from scintillator. Absolute neutron flux measured.	$\sigma_{n,2n}(D)$ = 0.2 ± 0.02 barn. Owing to efficiency errors, accuracy of cross-section determination ~ 5%. Detector efficiency determined with spontaneous fission source - ^{244}Cm (ν = 2.81 ± 0.059) or ^{252}Cf (ν = 3.869 ± 0.078) placed at centre of detector.

Table 6 (continued)

Work	Author(s)	Laboratory	Where and when published	Neutron source	Energy E (MeV)	E (MeV)	Detector	Method	Comments
N-2	Citron A.C., Goldberg M.D., Hill R.W., Le Blanc J.M., Haering J.P.	University of California	Phys. Rev., 123,218 (1961)	T(p,n) $\quad$ D(d,n)	6,11;6,55 7,32;8,26 $\quad$ 10,2;14,1	— $\quad$ —	See. [N-1]	See [N-1]	$\sigma_D(14.1) = 0.18 \pm 0.02$ barn. ^{244}Cm ($\nu = 2.75$) and ^{252}Cf ($\nu = 3.8$). Owing to correction for thickness of target, accuracy of cross-section determination $\leq 5\%$; owing to correction for presence of low-energy neutrons in incident beam, accuracy of cross-section determination $\sim 5\%$ (see also Ref. [N-1]).
N-3	Holmberg M., Hansen J.	Stockholm	Conference on Nuclear Data for Reactors, Paris 17-21 October 1966, paper CN-23/18.	D(d,n)	4,1 + 6,6	—	Large liquid scintillator	Method based on the time correlation between pulses corresponding to each of the two neutrons	$\sigma_{n,2n}$ at 6.5 MeV measured with an accuracy of $\sim 10\%$. Efficiency determined in relation to $\nu(^{252}$Cf).
N-4	Holmberg M.	Stockholm	N.P., A123,327 (1968)	D(d,n)	4,0 +6,55	—	See [N-3]	See [N-3]	$\sigma_{n,2n}(6.0$ MeV) measured with an accuracy of 10%. Efficiency determined in relation to $\nu(^{252}$Cf).
N-5	Shirato S., Koori	St. Paul's University Tokyo	N.P., A120,387 (1968)	T(d,n)	14,1	0,15	Telescope of three counters with Si(Li) detector	Angular distribution of breakdown neutrons measured	$\sigma_{n,2n}(14,1)=0,18 \pm 0,007$ barn (from the difference $\sigma_t - \sigma_{el}$). $\int_0^{90} \sigma_{in}(\theta_{lab})=0,155 \pm 0,006$ barn
N-6	Seagrave J.D., Hopkins J.C., Dixon D.R., Kenton R.W., Kerr E.C., Niiler A., Sherman R.H., Walter R.L.	LASL	A.P., 74,250 (1972)	D(d,n)	18,55 20,5 23,0	—	Large liquid scintillator	Absolute value of differential cross-section for elastic scattering measured	$\sigma_t(D)$ barn $\quad$ $\sigma_{el}(D)$ barn $\quad$ $\sigma_n(D)$ barn $0,643\pm0,012$ $\quad$ $0,186\pm0,02$ $\quad$ $0,157\pm0,041$ $0,586\pm0,01$ $\quad$ $0,442\pm0,04$ $\quad$ $0,144\pm0,037$ $0,523\pm0,0$ $\quad$ $0,3\pm0,0$ $\quad$ $0,1\pm0,0$ Normalized to $\sigma(H)$.

- 33 -

Fig. 1a: Total cross-section of deuterium

Fig. 1b: Total cross-section of deuterium
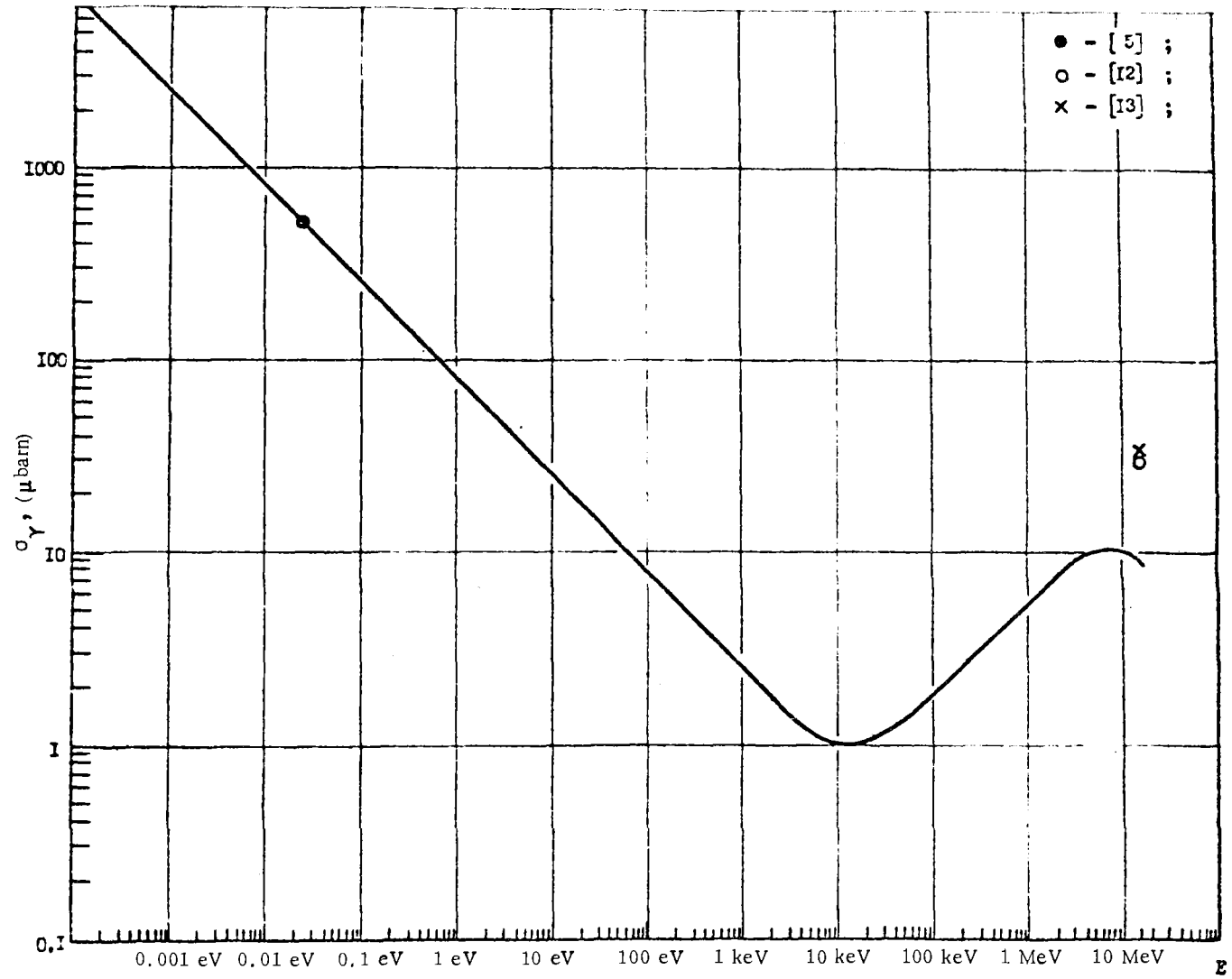
Fig. 2: Cross-section for the radiative capture of neutrons by deuterium
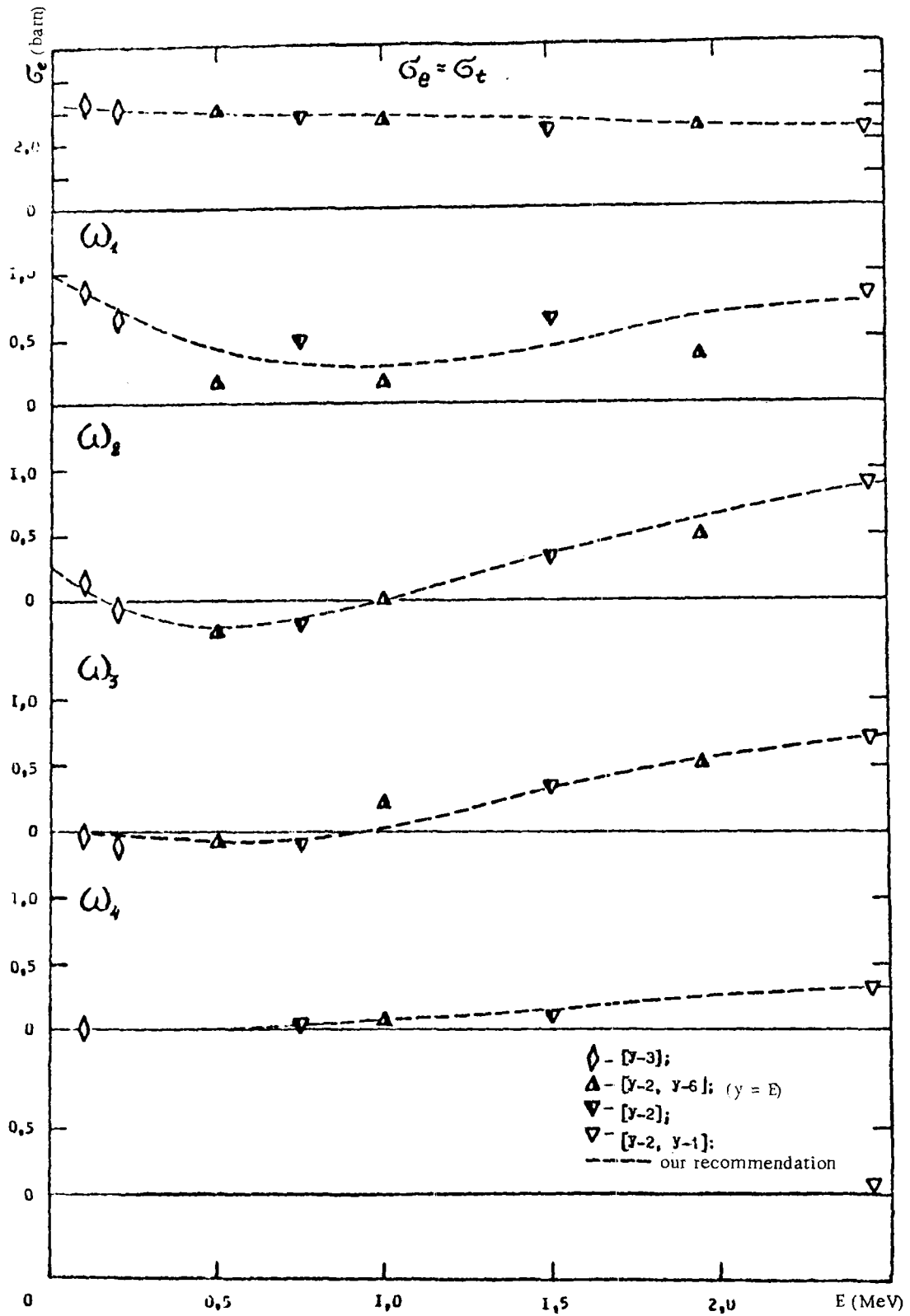
Fig. 3a: Angular momenta of neutrons elastically scattered by deuterium
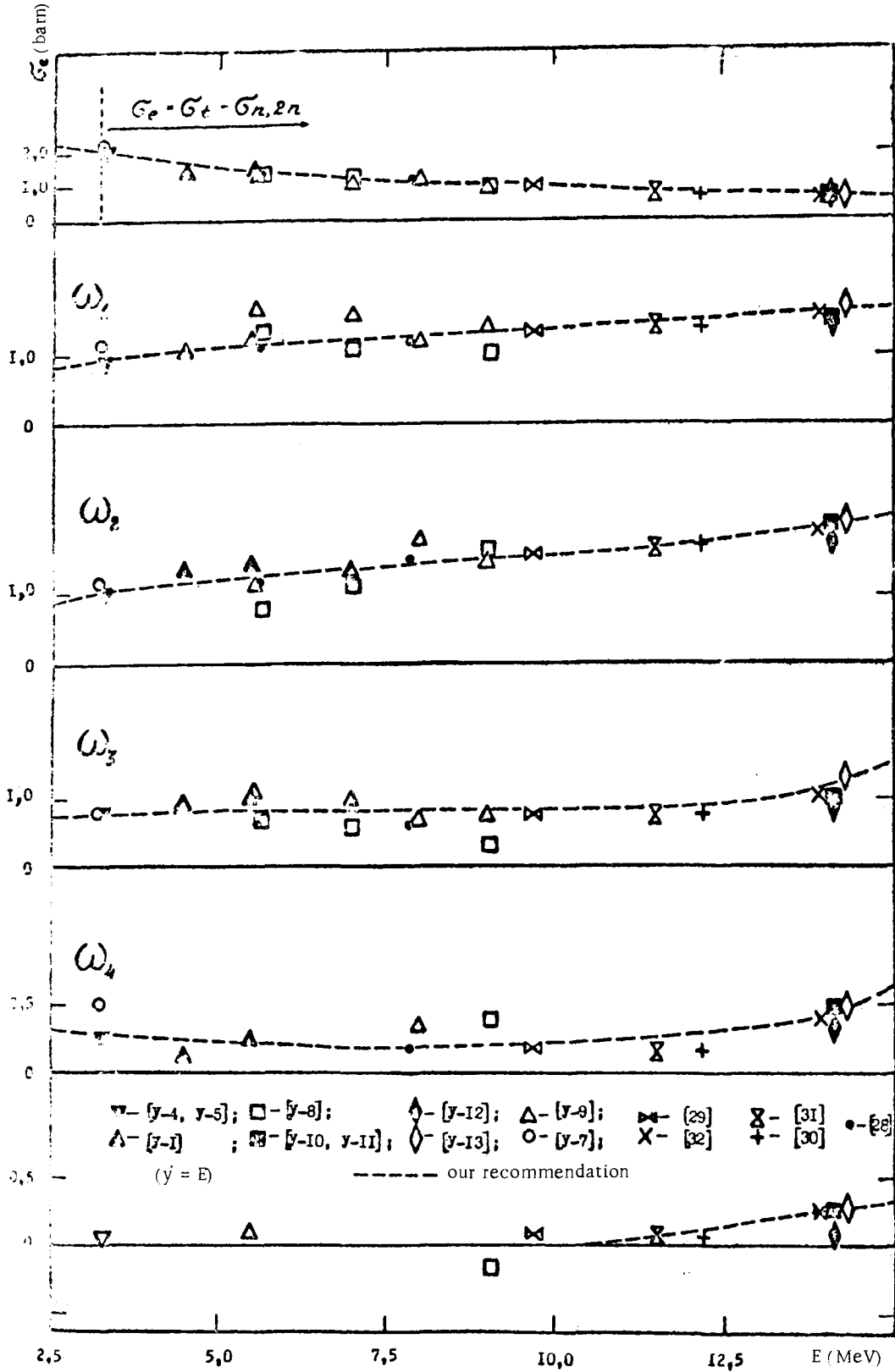
Fig. 3b: Angular momenta of neutrons elastically
scattered by deuterium
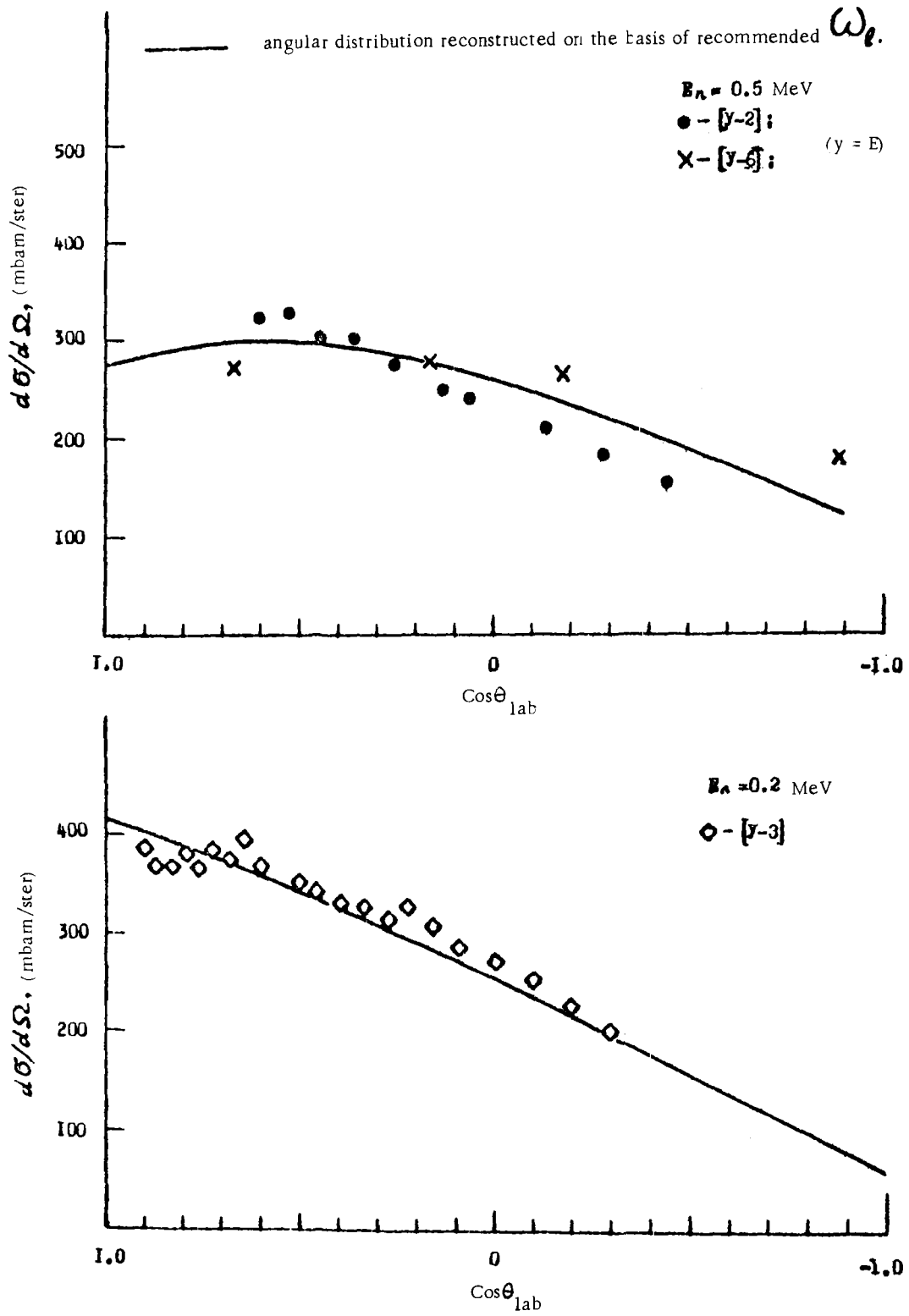
Fig. 4a: Angular distributions of neutrons elastically
scattered by deuterium
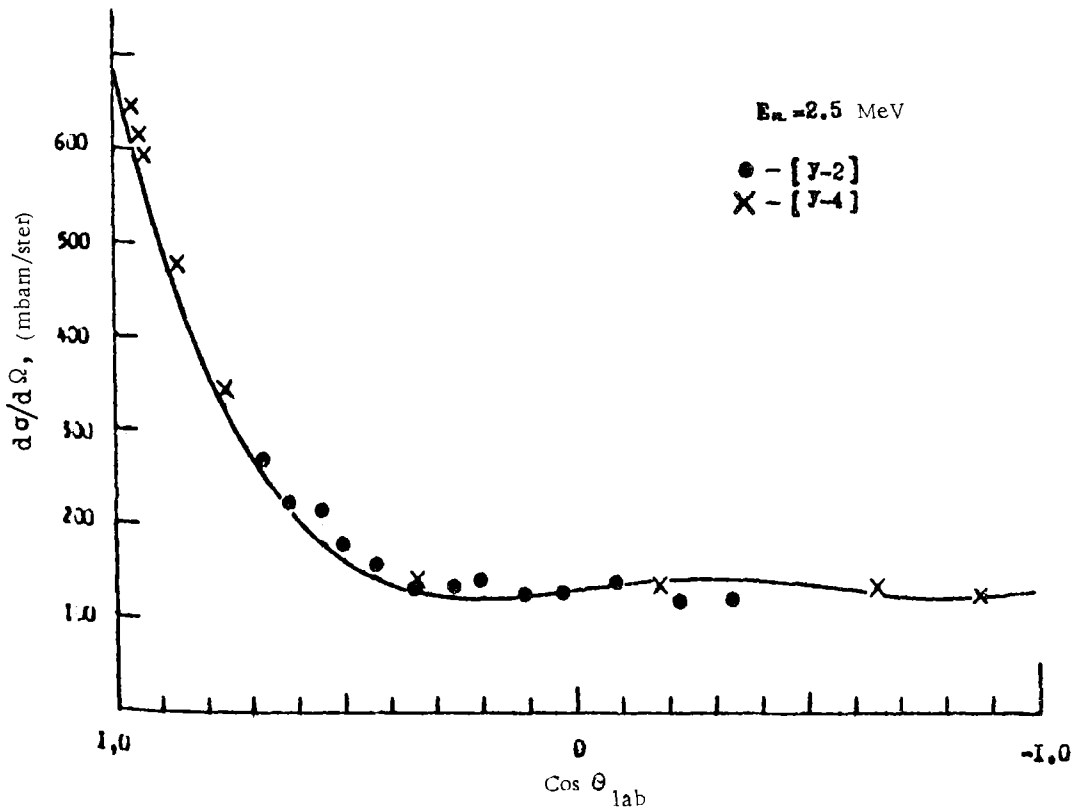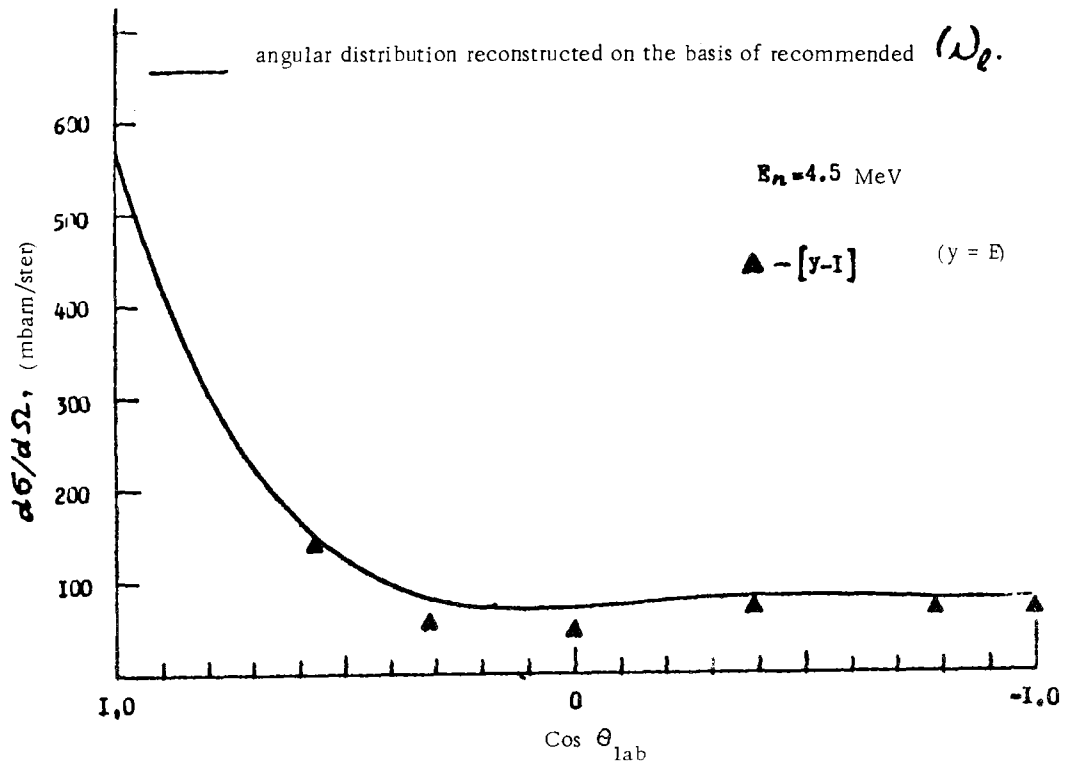
Fig. 4b: Angular distributions of neutrons elastically scattered by deuterium
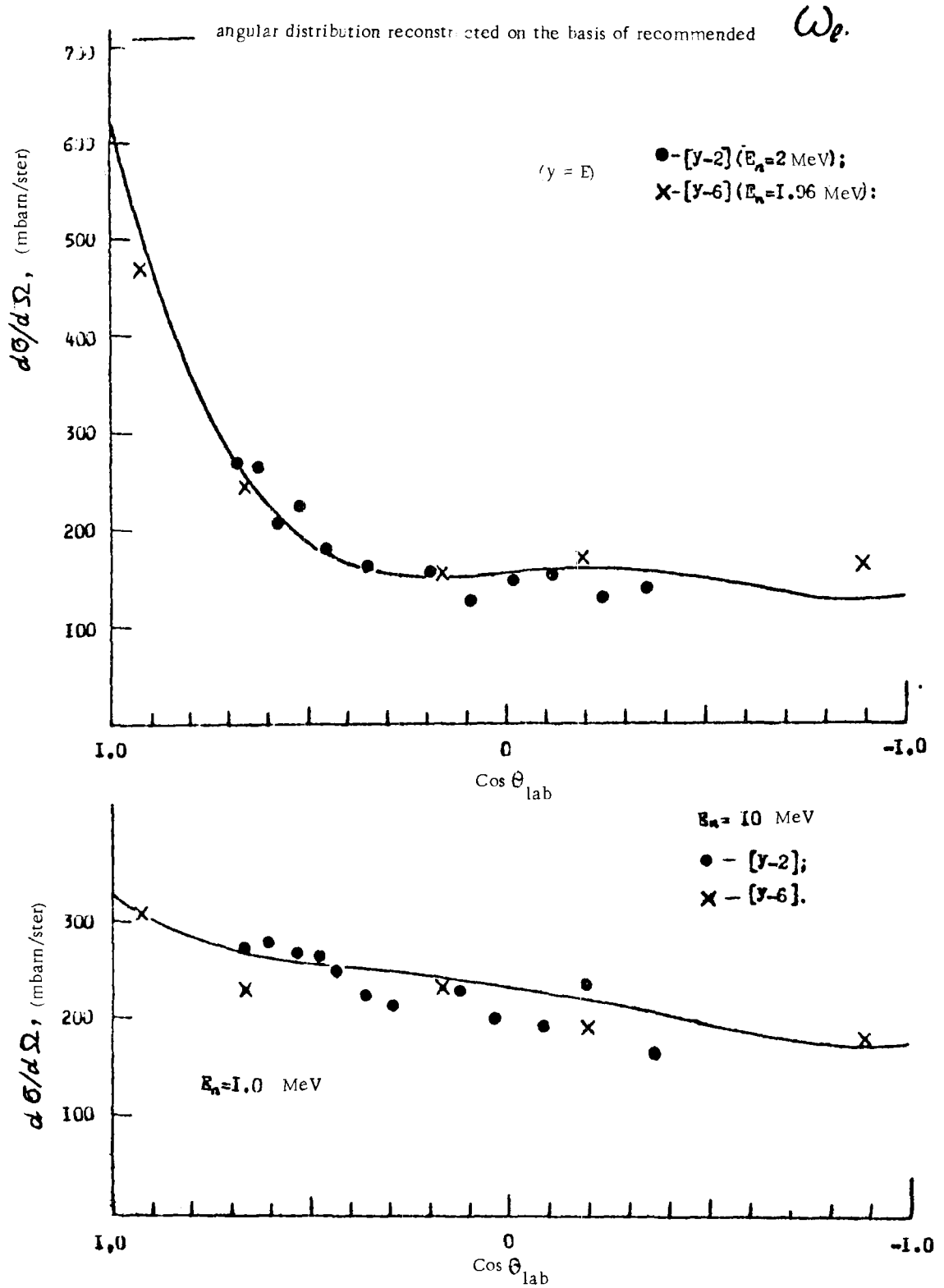
Fig. 4c : Angular distributions of neutrons elastically scattered by deuterium
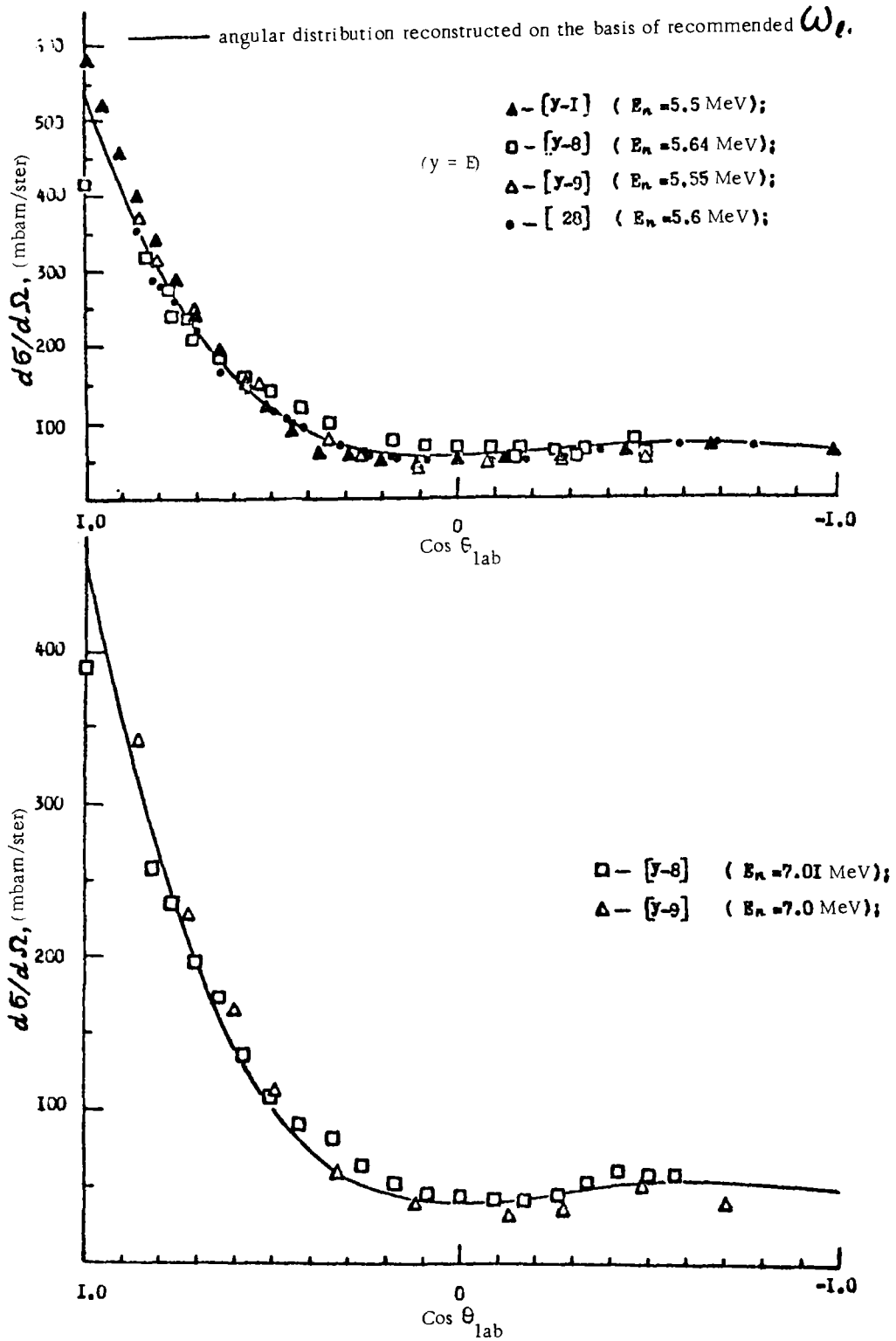
Fig. 4d: Angular distributions of neutrons elastically scattered by deuterium

angular distribution reconstructed on the basis of recommended ω_f.

$d\sigma/d\Omega$, (mbarn/ster)

300

200

100

(y = E)

△ - (Y-9)
■ - (Y-10, Y-11) } (E_n=14.1 MeV);
◆ - (Y-12)

◊ - (Y-13) (E_n=14.3 MeV);

✕ - (32)(E_n=13.93 MeV);

1.0

0

Cos θ$_{lab}$

-1.0

$d\sigma/d\Omega$, (mbarn/ster)

300

200

100

□ - (Y-8)(E_n=9.04 MeV);
△ - (Y-9)(E_n=9.0 MeV);

1.0

0

Cos θ$_{lab}$

-1.0
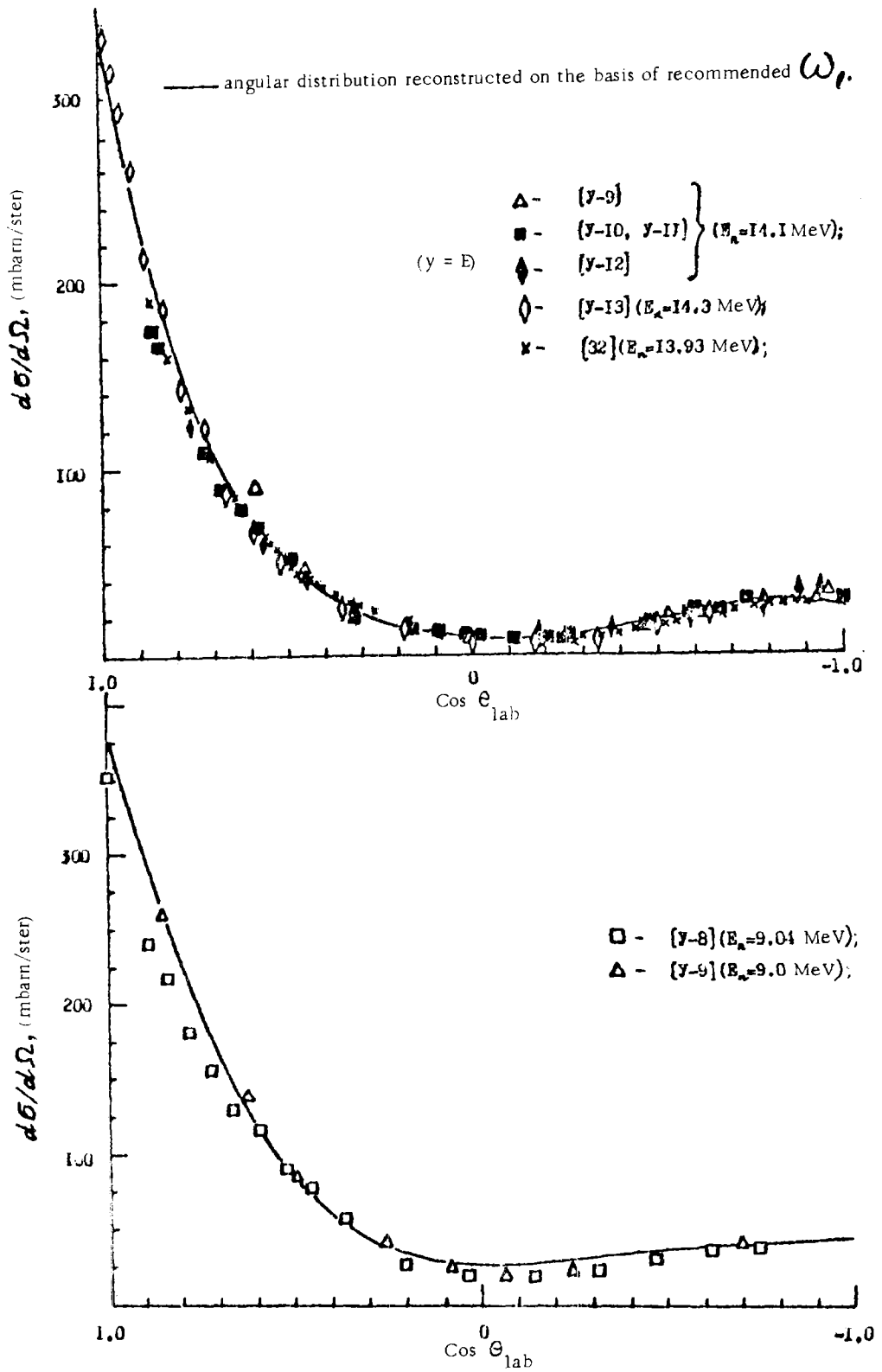
Fig. 4e: Angular distributions of neutrons elastically scattered by deuterium
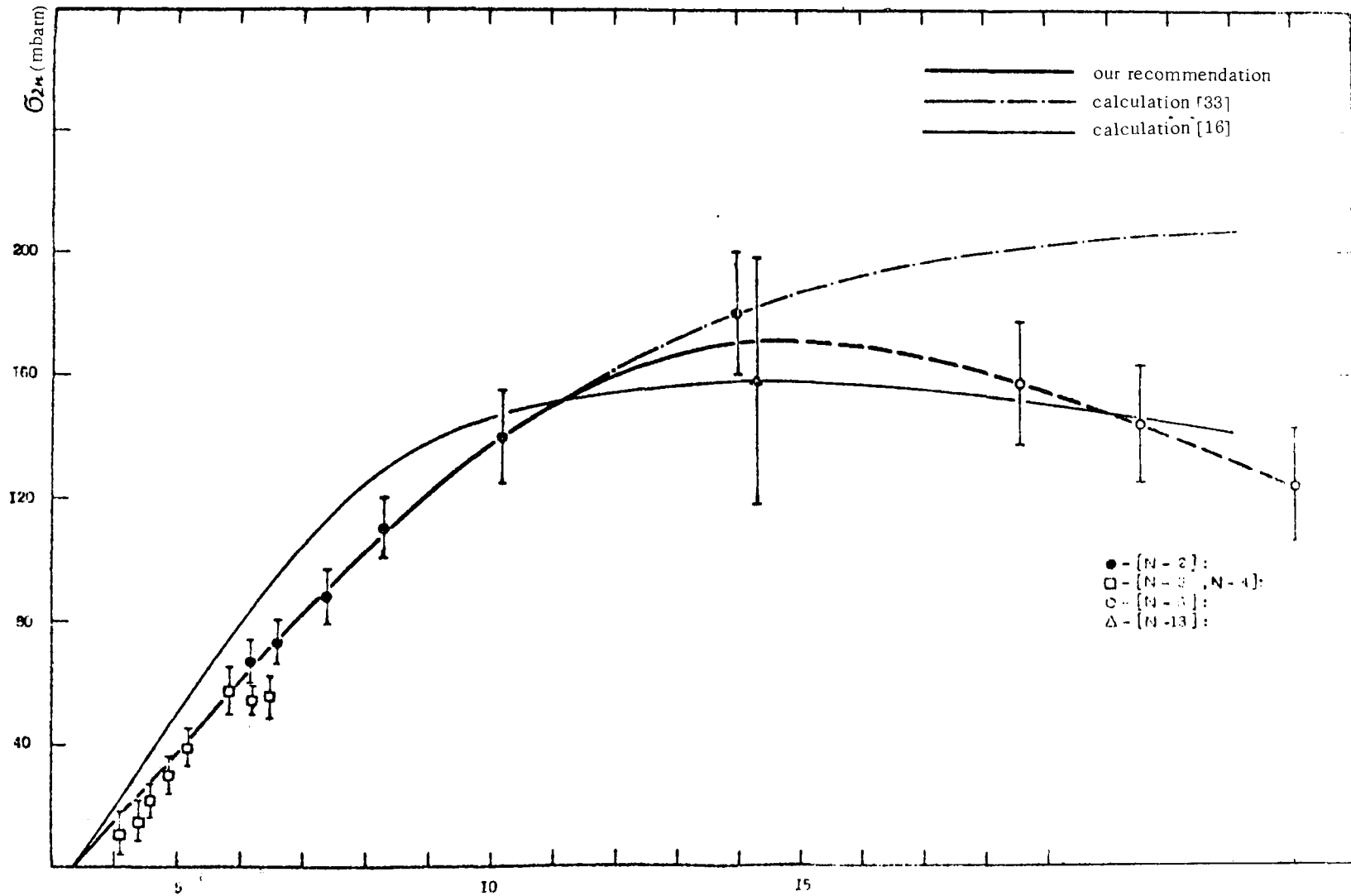
Fig. 5: Cross-section for the reaction (n, 2n)
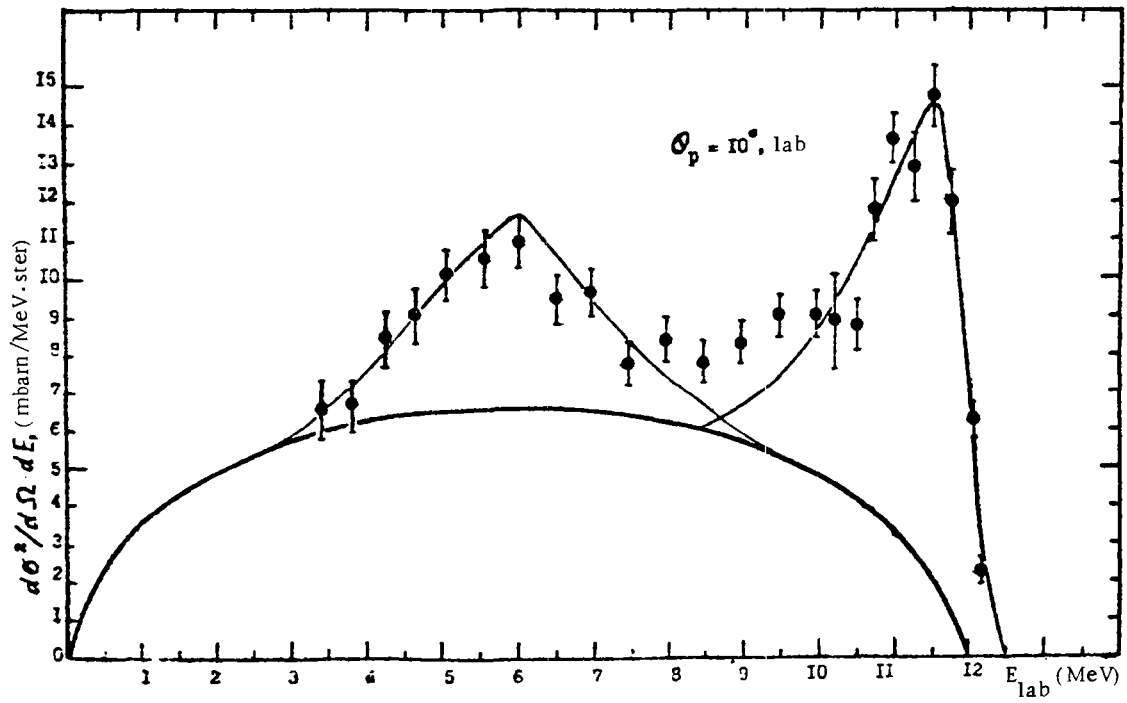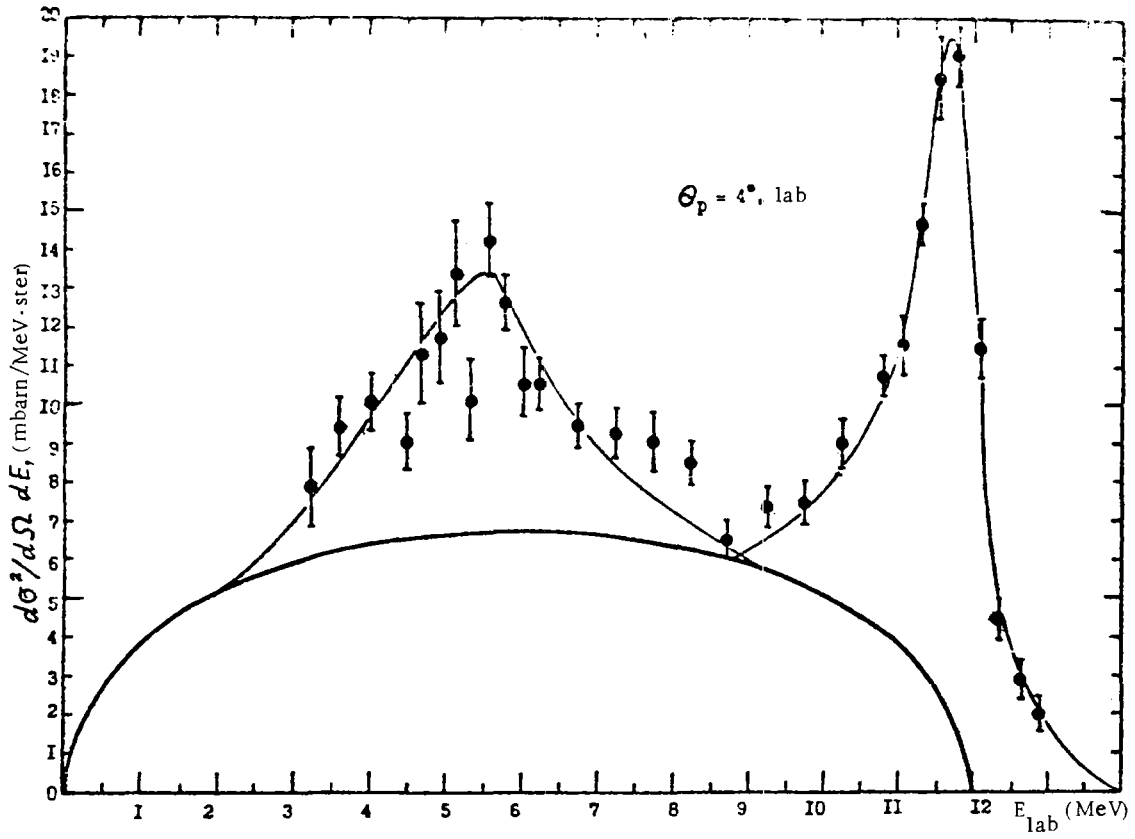
Fig. 7a: Spectra of photons formed at various angles in the reaction D(n, 2n)p
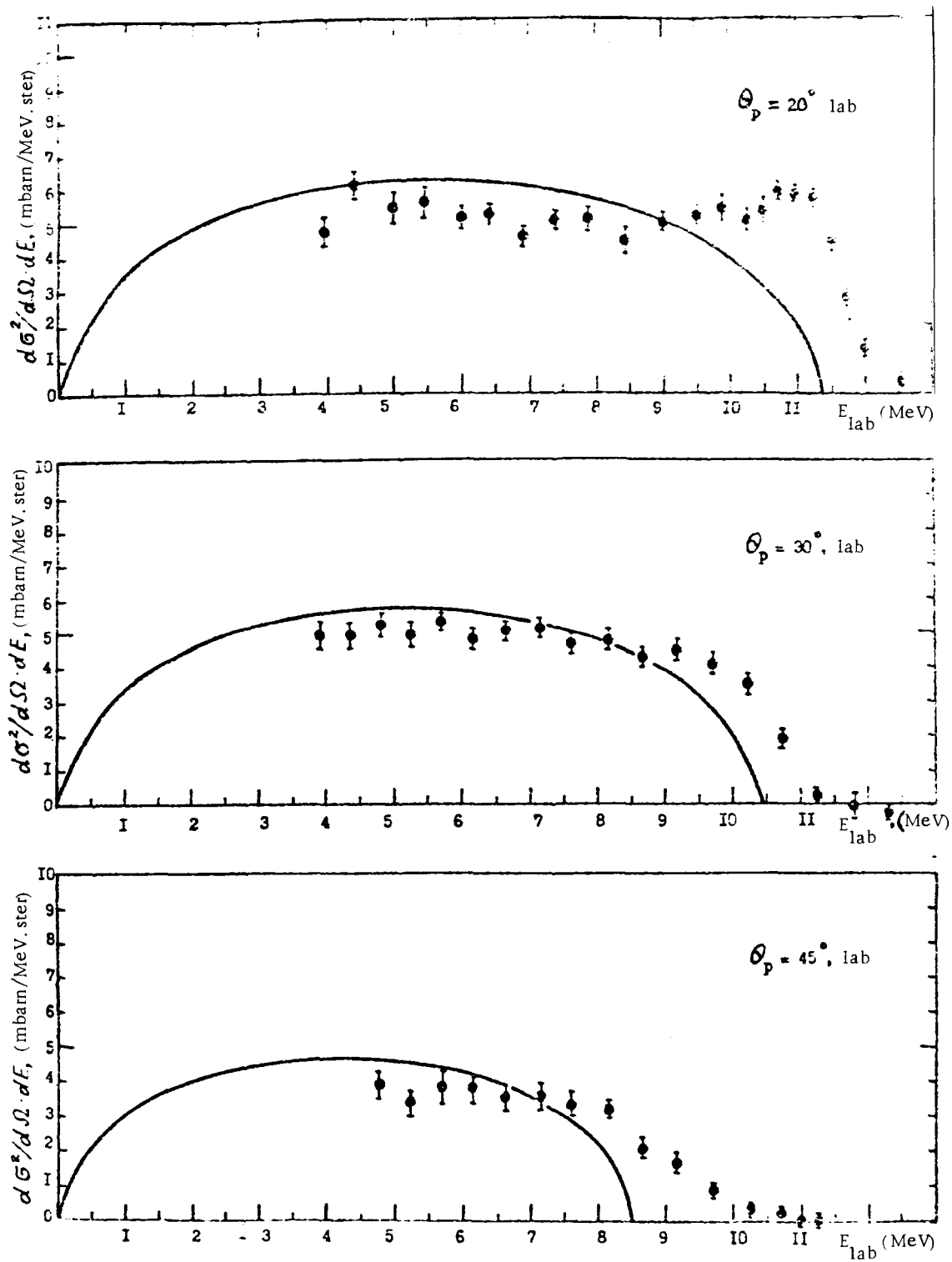
Fig. 7b: Spectra of photons formed at various angles in the reaction D(n, 2n)p
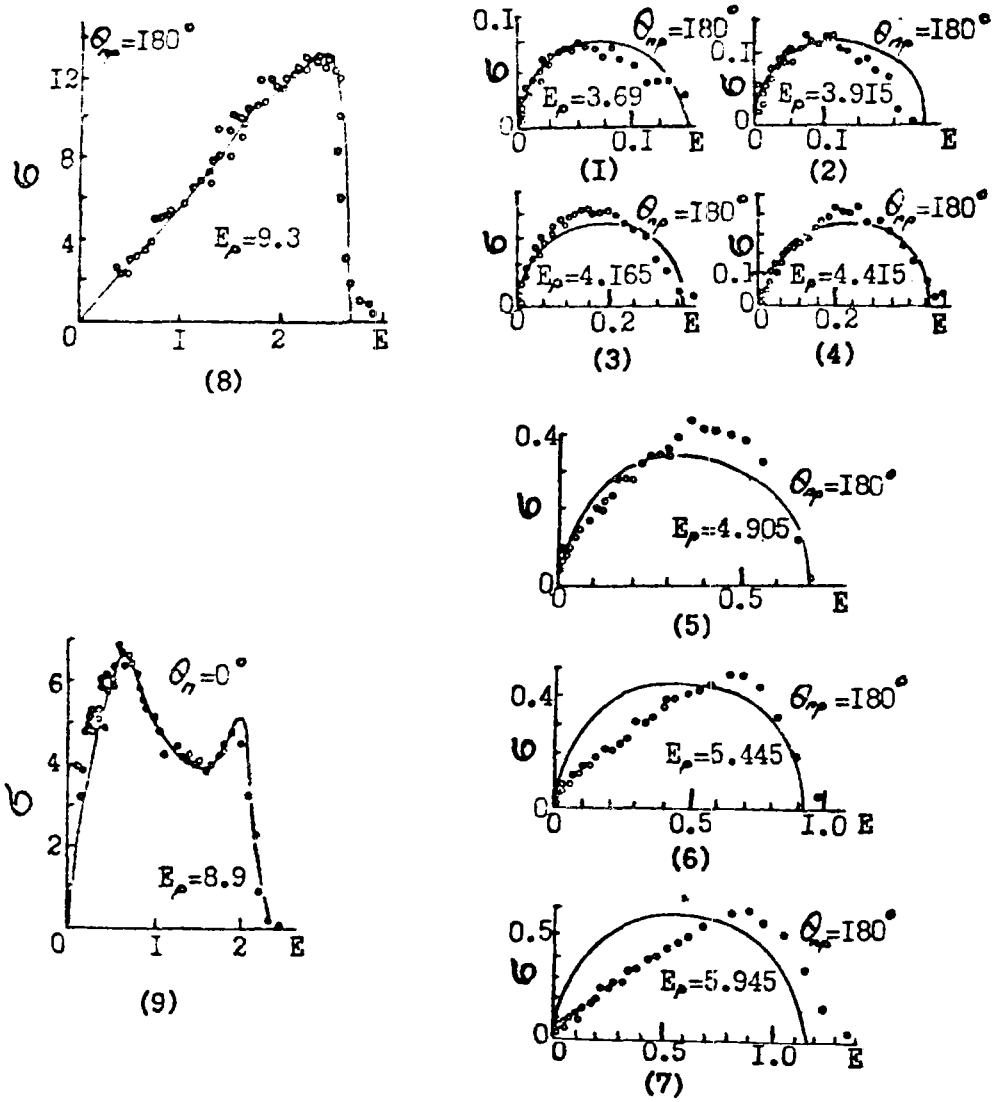
Fig. 8: Spectra of neutrons from the reactor p + d → n + p + p. Spectrum (9) was obtained in the reaction D(p,n) at an angle of 0° to the incident neutron beam. Spectra (1)-(8) were obtained in H(d,n) reactions at an angle of 0° to a beam of deuterons of energy E_d. These spectra are regarded here as the spectra of neutrons escaping at an angle of 180° to the proton beam in the reaction D(p,n) produced by protons with energy $E_p = E_d/2$. The E_p values (in MeV) are given on the graphs. Spectra (1)-(7) were obtained in Ref. [20], spectrum (8) in Ref. [36] and spectrum (9) in Ref. [35]. Along the abscissa - the scattered neutron energy E in centre-of-mass system; along ordinate - the cross section σ_{2n} in relative units. On graphs (1)-(7), the continuous curves are breakdown spectra; on graphs (8) and (9) they are spectra which take into account direct interactions.

θ_n and θ_{np} denote angle to incident particle beam.
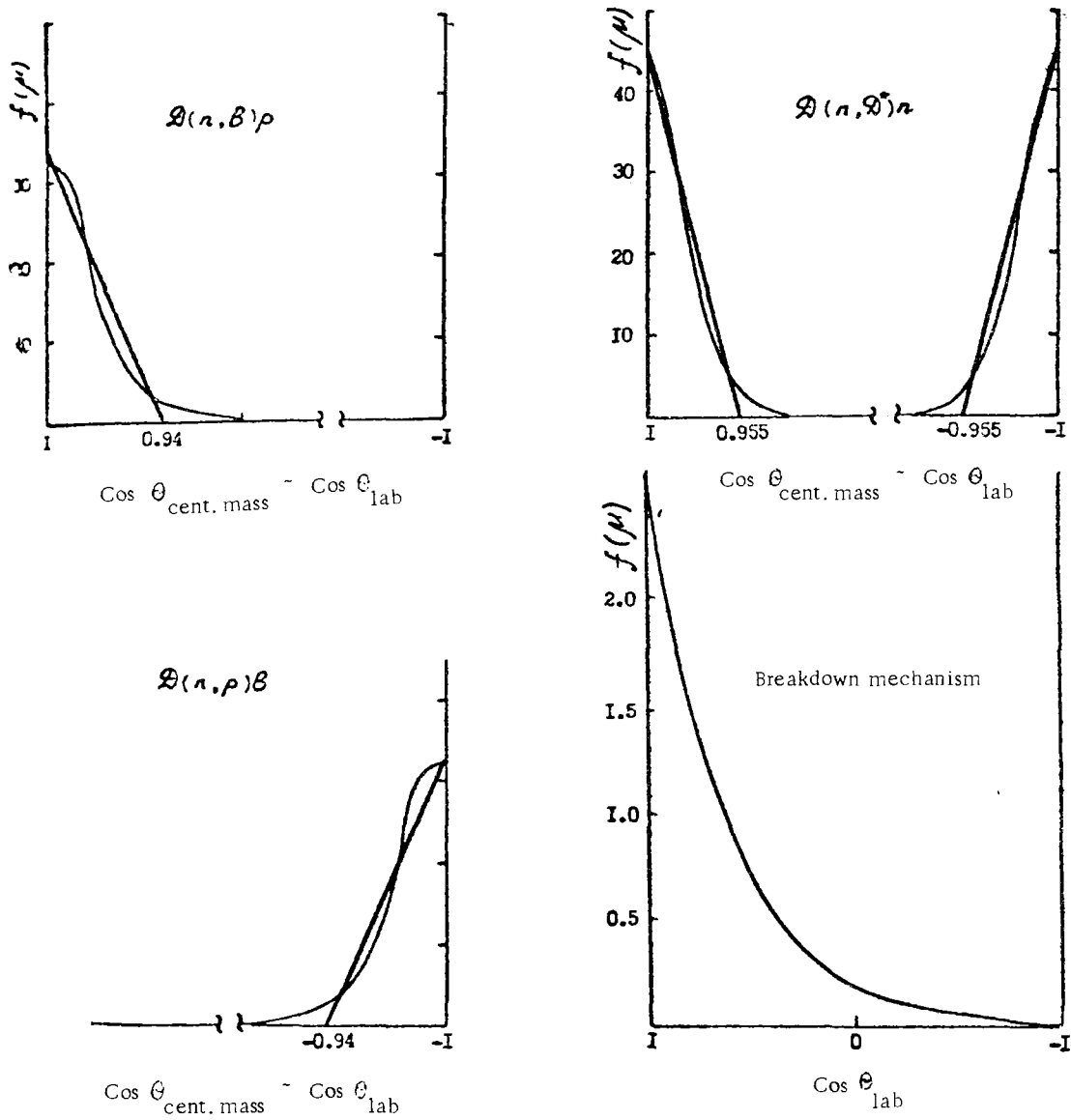
Fig. 9: Angular distributions f(μ) of neutrons from the reaction D(n, 2n) occurring by different mechanisms, $\int_{-1}^{1} f(\mu) d\mu = 1$

ANNEX 1

System of 26 group constants for deuterium.

Matrices of the angular momenta of intergroup transitions of the cross-section for the elastic scattering of neutrons by deuterium.

Matrices of the angular momenta of intergroup transitions of the cross-section for the reaction $D(n,2n)H$.

Table 7 [*]/

System of 26 group constants for deuterium

E_i	Δu	σ_t	σ_c	σ_{in}	σ_e	μ
14 MeV		0,820	0,0000	0,170	0,650	0,541
10,5-14,0	0,28	0,959	0,0000	0,154	0,805	0,408
6,5 -10,5	0,48	1,274	0,0000	0,094	1,180	0,417
4,0 - 6,5	0,48	1,658	0,0000	0,034	1,624	0,357
2,5 - 4,0	0,48	2,110	0,0000	0,002	2,108	0,299
1,4 - 2,5	0,57	2,564	0,0000		2,564	0,199
0,8 - 1,4	0,57	2,854	0,0000		2,854	0,109
0,4 - 0,8	0,69	2,947	0,0000		2,94	0,131
0,2 - 0,4	0,69	3,050	0,0000		3,050	0,209
0,1 - 0,2	0,69	3,161	0,0000		3,161	0,269
46,5-100 keV	0,77	3,255	0,0000		3,255	0,300
21,5-46,5	0,77	3,319	0,0000		3,319	0,318
10,0-21,5	0,77	3,356	0,0000		3,356	0,328
4,65-10,0	0,77	3,374	0,0000		3,374	0,332
2,15-4,65	0,77	3,382	0,0000		3,382	0,333
1,0 -2,15	0,77	3,386	0,0000		3,386	0,333
465 -1000 eV	0,77	3,388	0,0000		3,388	0,333
215 - 465	0,77	3,389	0,0000		3,389	0,333
100 - 215	0,77	3,390	0,0000		3,390	0,333
46,5- 100	0,77	3,390	0,0000		3,390	0,333
21,5-46,5	0,77	3,390	0,0000		3,390	0,333
10,0-21,5	0,77	3,390	0,0000		3,390	0,333
4,65-10,0	0,77	3,390	0,0000		3,390	0,333
2,15-4,65	0,77	3,390	0,0000		3,390	0,333
1,0 -2,15	0,77	3,390	0,0000		3,390	0,333
0,465-1,0	0,77	3,3901	0,0001		3,390	0,333
0,215-0,465	0,77	3,3902	0,0002		3,390	0,333
0,0252	--	3,3905	0,0005		3,390	0,333

[*]/ All cross-sections in Table 7 are in barns.

Table 8

Matrices of the angular momenta of intergroup transitions of the
cross-section for the elastic scattering of neutrons
by deuterium

		$\dfrac{B_0^i \text{ from } i \text{ in } i+k}{B_0^i}$ for k =						
i	E_i ,MeV	0	1	2	3	4	5	$\mathcal{B}_0^i/\mathcal{B}_0^i$
-1	14,0	0,0113	0,5599	0,2307	0,0466	0,0491	0,1034	1,0000
0	10,5	0,1091	0,5070	0,1103	0,0529	0,1129	0,0278	1,0000
1	6,5	0,2445	0,4079	0,1058	0,1122	0,1232	0,0064	1,0000
2	4,0	0,2773	0,3275	0,1404	0,1432	0,1116		1,0000
3	2,5	0,2779	0,3146	0,1523	0,2051	0,0501		1,0000
4	1,4	0,2696	0,2545	0,2462	0,2089	0,0208		1,0000
5	0,8	0,1795	0,3363	0,2894	0,1900	0,0043		1,0000
6	0,4	0,1967	0,3721	0,2911	0,1398	0,0003		1,0000
7	0,2	0,2309	0,3960	0,2371	0,0980			1,0000
8	0,1	0,2659	0,4371	0,2420	0,0550			1,0000
9	0,0465	0,3216	0,4304	0,2027	0,0453			1,0000
10	0,0215	0,3402	0,4198	0,1944	0,0456			1,0000
11	0,01	0,3385	0,4208	0,1957	0,0450			1,0000
12	0,00465	0,3338	0,4227	0,1936	0,0449			1,0000

		$\dfrac{B_1^i \text{ from } i \text{ in } i+k}{B_0^i}$ for k =						
i	E_i ,MeV	0	1	2	3	4	5	$\mathcal{B}_1^i/\mathcal{B}_1^i$
-1	14,0	0,0389	1,4000	0,3893	0,0155	-0,0545	-0,2413	1,6220
0	10,5	0,5330	1,1536	0,1041	-0,0257	-0,2234	-0,0777	1,4630
1	6,5	0,6669	0,8814	0,0810	-0,0892	-0,2892	-0,0186	1,3523
2	4,0	0,7431	0,6733	0,0695	-0,1533	-0,2625		1,0701
3	2,5	0,7302	0,5936	0,0134	-0,3181	-0,1321		0,8960
4	1,4	0,6900	0,4106	-0,0516	-0,3945	-0,0573		0,5981
5	0,8	0,4502	0,4463	-0,1518	-0,4057	-0,0123		0,3267
6	0,4	0,4616	0,4248	-0,1924	-0,3000	-0,0009		0,3931
7	0,2	0,5465	0,4694	-0,2004	-0,1877			0,6279
8	0,1	0,6343	0,5009	-0,2043	-0,1245			0,8064
9	0,0465	0,7548	0,4738	-0,1933	-0,1037			0,9466
10	0,0215	0,7991	0,4764	-0,1713	-0,1042			1,0000
11	0,010	0,7964	0,4793	-0,1727	-0,1030			1,0000
12	0,00465	0,7969	0,4788	-0,1727	-0,1030			1,0000

Table 8 (continued)

| ℓ | E_ℓ, MeV | \multicolumn{6}{c}{$\dfrac{B_2^i \text{ from } i \text{ in } i+k}{B_0^i}$ for k =} | $\mathcal{B}_2^i/\mathcal{B}_0^i$ |

ℓ	E_ℓ, MeV	0	1	2	3	4	5	$\mathcal{B}_2^i/\mathcal{B}_0^i$
-1	14,0	0,0563	1,3863	-0,0062	-0,1070	-0,0638	0,2231	1,9887
0	10,5	0,7833	0,9890	-0,1797	-0,1145	0,1082	0,1125	1,6928
1	6,5	0,9160	0,6382	-0,1940	-0,1945	0,2038	0,0288	1,3983
2	4,0	0,9826	0,4191	-0,2826	-0,1754	0,2503		1,1943
3	2,5	0,9603	0,2363	-0,3406	-0,0321	0,1673		0,9917
4	1,4	0,8235	0,0043	-0,5099	0,1621	0,0793		0,5648
5	0,8	0,5115	-0,2143	-0,5460	0,2920	0,0190		0,0622
6	0,4	0,4453	-0,3502	-0,4865	0,2218	0,0014		-0,1682
7	0,2	0,5399	-0,3359	-0,4568	0,1449			-0,1079
8	0,1	0,6406	-0,3827	-0,3412	0,1067			0,0234
9	0,0465	0,7352	-0,3809	-0,2594	0,0923			0,1872
10	0,0215	0,7799	-0,3598	-0,2534	0,0922			0,2589
11	0,0100	0,7803	-0,3587	-0,2548	0,0921			0,2589
12	0,00465	0,7804	-0,3637	-0,2499	0,0921			0,2589

| i | E_i, MeV | \multicolumn{6}{c}{$\dfrac{B_3^i \text{ from } i \text{ in } i+k}{B_0^i}$ for k =} | $\mathcal{B}_3^i/\mathcal{B}_0^i$ |

i	E_i, MeV	0	1	2	3	4	5	$\mathcal{B}_3^i/\mathcal{B}_0^i$
-1	14,0	0,0793	1,6796	-0,5562	-0,0496	0,1325	-0,0721	1,2125
0	10,5	0,9044	0,1909	-0,2749	0,0775	0,1141	-0,1261	0,8859
1	6,5	0,9515	-0,0723	-0,2218	0,2248	0,0013	-0,0360	0,8475
2	4,0	0,9567	-0,1808	-0,1903	0,3342	-0,1061		0,8137
3	2,5	0,9062	-0,3308	-0,0396	0,3640	-0,1481		0,7517
4	1,4	0,6771	-0,4192	0,1305	0,1933	-0,0339		0,4973
5	0,8	0,3696	-0,6385	0,3638	0,0026	-0,0235		0,0740
6	0,4	0,2129	-0,6586	0,4005	-0,0145	-0,0019		-0,0616
7	0,2	0,2808	-0,6914	0,3897	-0,0141			-0,0350
8	0,1	0,3564	-0,7177	0,3704	-0,0266			-0,0175
9	0,0465	0,3807	-0,6586	0,3019	-0,0298			-0,0058
10	0,0215	0,4065	-0,6552	0,2726	-0,0299			0,0000
11	0,0100	0,4101	-0,6598	0,2807	-0,0310			0,0000
12	0,00465	0,4098	-0,6594	0,2806	-0,0310			0,0000

Table 8 (continued)

E_i, MeV	

$\dfrac{B_4^i \text{ from } i \text{ in } i+k}{B_0^i}$ for k =

E_i, MeV	0	1	2	3	4	5	$\mathcal{B}_4^i/\mathcal{B}_c^i$
14,0	0,0937	1,0074	-0,6603	0,1171	-0,0314	-0,009?	0,4305
10,5	0,8320	-0,6326	0,0244	0,1078	-0,2320	0,1171	0,2758
6,5	0,8079	-0,6572	0,0955	0,0570	-0,1673	0,0397	0,2056
4,0	0,7310	-0,5880	0,2176	-0,0560	-0,0540		0,2506
2,5	0,6526	-0,5339	0,3507	-0,2610	0,0896		0,2980
1,4	0,3751	-0,3662	0,4354	-0,2379	0,0705		0,2269
0,8	0,1410	-0,2685	0,3744	-0,1959	0,0255		0,0765
0,4	-0,0298	-0,1005	0,2585	-0,1184	0,0023		0,0121
0,2	-0,0006	-0,1457	0,2284	-0,0821			0,0000
0,1	0,0343	-0,1152	0,1269	-0,0460			0,0000
0,0465	0,0212	-0,0912	0,0830	-0,0290			-0,0060
0,0215	0,0260	-0,1030	0,0961	-0,0280			-0,0089
0,0100	0,0289	-0,1070	0,0856	-0,0266			-0,0089
0,00465	0,0285	-0,1016	0,0908	-0,0266			-0,0089

$\dfrac{B_5^i \text{ from } i \text{ in } i+k}{B_0^i}$ for k =

E_i, MeV	0	1	2	3	4	5	$\mathcal{B}_5^i/\mathcal{B}_c^i$
14,0	0,1204	0,1844	-0,1916	0,0825	-0,1174	0,1756	0,2539
10,5	0,7713	-0,9588	0,3041	-0,1153	0,1654	-0,0805	0,0772
6,5	0,5695	-0,7326	0,2695	-0,2413	0,1746	-0,0305	0,0002
4,0	0,4311	-0,5346	0,2314	-0,2493	0,1213		-0,0001
2,5	0,3394	-0,2984	0,0059	-0,0750	-0,0210		0,0000
1,4	0,1010	-0,0163	-0,1358	0,0363	-0,0452		0,0000
0,8	-0,0352	0,2459	-0,3460	0,1616	-0,0248		0,0000
0,4	-0,1210	0,3405	-0,3039	0,0914	-0,0025		0,0000
0,2	-0,1184	0,3234	-0,2910	0,0760			0,0000
0,1	-0,1153	0,3192	-0,2636	0,0597			0,0000
0,0465	-0,1114	0,2620	-0,1930	0,0433			0,0000
0,0215	-0,1172	0,2642	-0,1982	0,0412			0,0000
0,0100	-0,1179	0,2665	-0,1806	0,0409			0,0000
0,00465	-0,1182	0,2669	-0,1896	0,0409			0,0000

Table 9

Matrices of group angular momenta for the D(n,2n) reaction

$\dfrac{B_0 \text{ from } i \text{ in } i+k}{B_0^i}$ for k =

i	E, MeV	0	I	2	3	4	5	6	7	8	9	IC
-I	14,0-14,1	-	0,0063	0,2074	0,3299	0,2007	0,1296	0,0638	0,0290	0,0105	0,0037	0,0171
0	10,5-14,0	0,0002	0,0709	0,2540	0,2465	0,2007	0,1090	0,0689	0,0351	0,0094	0,0005	0,0018
I	6,5-10,5	0,0012	0,0525	0,2137	0,3022	0,2005	0,1344	0,0583	0,0236	0,0092	0,0030	0,0014
2	4,0-6,5	0,0000	0,0197	0,1582	0,2908	0,2873	0,1451	0,0610	0,0252	0,0096	0,0028	0,0019
3	2,5-4,0	-	0,0003	0,00829	0,3534	0,3050	0,1531	0,0693	0,0243	0,0080	0,0029	0,0011

$\dfrac{B_1 \text{ from } i \text{ in } i+k}{B_0^i}$ for k =

i	E, MeV	0	I	2	3	4	5	6	7	8	9	IC
-I	14,0-14,1	-	0,0586	0,6330	0,7988	0,4447	0,2833	0,1030	0,0630	0,0227	0,0081	-0,0440
0	10,5-14,0	0,0026	0,2971	0,6623	0,5375	0,3535	0,1504	0,0544	-0,0077	0,0071	0,0026	0,0018
I	6,5-10,5	0,0130	0,2447	0,5967	0,7089	0,3981	0,2113	0,0734	0,0233	0,0036	0,0027	0,0012
2	4,0-6,5	0,0010	0,0899	0,4921	0,7737	0,6954	0,3256	0,1289	0,0501	0,0160	0,0049	0,0021
3	2,5-4,0	-	0,0079	0,3660	0,1110	0,7984	0,2993	0,1012	0,0295	0,0098	0,0027	0,0013

$\dfrac{B_2 \text{ from } i \text{ in } i+k}{B_0^i}$ for k =

i	E, MeV	0	I	2	3	4	5	6	7	8	9	IC
-I	14,0-14,1	-	0,0697	0,5676	0,6300	0,2552	0,1549	0,1007	0,0333	0,0119	0,0042	0,0770
0	10,5-14,0	0,0034	0,3292	0,6125	0,3624	0,1233	0,0243	0,0297	0,0523	0,0018	0,0003	0,0000
I	6,5-10,5	0,0192	0,3248	0,6812	0,6060	0,2306	0,0906	0,0223	0,0083	0,0026	0,0009	0,0004
2	4,0-6,5	0,0017	0,1300	0,8244	0,9776	0,7475	0,2998	0,1069	0,0393	0,0124	0,0039	0,0019
3	2,5-4,0	-	0,0131	0,5557	1,6252	1,2507	0,6137	0,2744	0,0955	0,0311	0,0100	0,0045

$\dfrac{B_3 \text{ from } i \text{ in } i+k}{B_0^i}$ for k =

i	E, MeV	0	I	2	3	4	5	6	7	8	9	IC
-I	14,0-14,1	-	-0,0000	-0,0001	0,2058	-0,0000	-0,0000	-0,0483	-0,0000	-0,0000	-0,0000	-0,1050
0	10,5-14,0	0,0052	03709	0,4969	0,7856	-0,0234	-0,0004	-0,0216	-0,0850	0,0005	0,0003	
I	6,5-10,5	0,0246	0,3596	0,5877	0,2873	0,0183	-0,0250	-0,0038	-0,0009	0,0008	0,0002	0,0001
2	4,0-6,5	0,0024	0,1475	0,7088	0,8279	0,5000	0,1535	0,0471	0,0168	0,0054	0,0017	0,0008
3	2,5-4,0	-										

$\dfrac{B_4 \text{ from } i \text{ in } i+k}{B_0^i}$ for k =

i	E, MeV	0	I	2	3	4	5	6	7	8	9	IC
-I	14,0-14,1	-	-0,0009	-0,0000	0,4599	-0,0000	-0,0000	0,0621	-0,0000	-0,0000	-0,0009	0,1250
0	10,5-14,0	0,0042	0,2066	0,2322	0,0779	0,0103	0,0158	0,0416	0,0930	0,0008	0,0003	0,0001
I	6,5-10,5	0,0249	0,3027	0,3159	0,0402	-0,0065	0,0151	0,0323	0,0113	0,0053	0,0004	0,0000
2	4,0-6,5	0,0031	0,1444	0,6426	0,5898	0,2392	0,0400	0,0076	0,0018	0,0002	0,0000	0,0000
3	2,5-4,0	-	0,0184	0,6761	1,8726	1,2795	0,4616	0,1553	0,0459	0,0138	0,0043	0,0019

$\dfrac{B_5 \text{ from } i \text{ in } i+k}{B_0^i}$ for k =

i	E, MeV	0	I	2	3	4	5	6	7	8	9	IC
-I	14,0-14,1	-	0,1293	0,1562	0,2646	-0,0175	-0,0094	-0,0798	-0,0019	-0,0006	-0,0003	-0,1675
0	10,5-14,0	0,0063	0,1821	0,1870	0,1589	0,0667	0,0173	-0,0365	-0,1024	0,0008	0,0003	0,0001
I	6,5-10,5	0,0267	0,2691	0,1686	0,0359	0,0717	0,0410	-0,0177	-0,0071	-0,0039	0,0004	0,0002
2	4,0-6,5	0,0038	0,1285	0,5033	0,3861	0,0037	0,0061	0,0016	0,0008	0,0004	0,0002	0,0001
3	2,5-4,0	-	0,0289	0,6980	1,6549	1,1477	0,2666	0,1132	0,0206	0,0111	0,0025	0,0015

ANNEX 2

Evaluated neutron data for deuterium in the SOCRATOR format

DEUTERIUM

200301002	235	5	1	2.000000	8	2003	0	1
1	1001	33	2	1102	33	2003	0	2
3	1002	33	4	2002	104	2003	0	3
5	3002	4	6	1016	15	2003	0	4
7	2016	4	8	3016	4	2003	0	5
1001	1	0.000000	0	0	0	2003	1	1
100000-09	150000+02	32	1	100000000	0	2003	1	2
0	1	31	0	0	0	2003	1	3
111	86	30	111000000	100000-09	339829+01	2003	1	4
250000-09	339524+01	500000-09	339371+01	750000-09	339302+01	2003	1	5
100000-08	339262+01	250000-08	339166+01	500000-08	339117+01	2003	1	6
750000-08	339096+01	100000-07	339083+01	250000-07	339052+01	2003	1	7
500000-07	339037+01	750000-07	339030+01	100000-06	339026+01	2003	1	8
250000-06	339017+01	500000-06	339012+01	750000-06	339010+01	2003	1	9
100000-05	339008+01	250000-05	339005+01	500000-05	339004+01	2003	1	10
750000-05	339003+01	100000-04	339003+01	250000-04	339002+01	2003	1	11
500000-04	339001+01	750000-04	339001+01	100000-03	339001+01	2003	1	12
250000-03	338961+01	500000-03	338900+01	750000-03	338830+01	2003	1	13
100000-02	338760+01	200000-02	338500+01	400000-02	338000+01	2003	1	14
600000-02	337600+01	800000-02	337200+01	100000-01	336700+01	2003	1	15
200000-01	334500+01	400000-01	330300+01	600000-01	326700+01	2003	1	16
800000-01	324000+01	100000+00	321500+01	133000+00	317000+01	2003	1	17
157000+00	313300+01	200000+00	310500+01	250000+00	307000+01	2003	1	18
300000+00	304000+01	350000+00	301500+01	400000+00	299500+01	2003	1	19
500000+00	296000+01	600000+00	293800+01	700000+00	292000+01	2003	1	20
800000+00	290500+01	900000+00	289000+01	100000+01	288000+01	2003	1	21
120000+01	283000+01	140000+01	276500+01	160000+01	270000+01	2003	1	22
180000+01	263000+01	200000+01	247000+01	230000+01	241000+01	2003	1	23
250000+01	230000+01	290000+01	218000+01	310000+01	212000+01	2003	1	24
333900+01	204000+01	350000+01	198000+01	400000+01	184000+01	2003	1	25
450000+01	173000+01	500000+01	163000+01	550000+01	154000+01	2003	1	26
600000+01	146000+01	650000+01	139000+01	700000+01	133000+01	2003	1	27
750000+01	125000+01	800000+01	123000+01	850000+01	118000+01	2003	1	28
900000+01	114000+01	950000+01	110000+01	100000+02	106000+01	2003	1	29
105000+02	102000+01	110000+02	990000+00	115000+02	960000+00	2003	1	30
120000+02	930000+00	125000+02	900000+00	130000+02	870000+00	2003	1	31
135000+02	840000+00	140000+02	820000+00	145000+02	800000+00	2003	1	32
150000+02	780000+00	000000-19	000000-19	000000-19	000000-19	2003	1	33

1112	1	0.000000	0	0	0	2003	2	1
100000-09	150000+02	32	1	100000000	0	2003	2	2
0	1	31	0	0	0	2003	2	3
111	86	30	111000000	100000-09	828700-02	2003	2	4
250000-09	324500-02	500000-09	370600-02	750000-09	302400-02	2003	2	5
100000-08	262100-02	250000-08	165700-02	500000-08	117200-02	2003	2	6
750000-08	956900-03	100000-07	828700-03	250000-07	524200-03	2003	2	7
500000-07	370500-03	750000-07	302500-03	100000-06	262100-03	2003	2	8
250000-06	165700-03	500000-06	117200-03	750000-06	957000-04	2003	2	9
100000-05	328700-04	250000-05	524100-04	500000-05	370600-04	2003	2	10
750000-05	302500-04	100000-04	262000-04	250000-04	165700-04	2003	2	11
500000-04	117200-04	750000-04	956000-05	100000-03	829000-05	2003	2	12
250000-03	324000-05	500000-03	371000-05	750000-03	303000-05	2003	2	13
100000-02	262000-05	200000-02	185000-05	400000-02	131000-05	2003	2	14
600000-02	112000-05	800000-02	103000-05	100000-01	100000-05	2003	2	15
200000-01	103000-05	400000-01	128000-05	600000-01	150000-05	2003	2	16
800000-01	172000-05	100000+00	194000-05	133000+00	225000-05	2003	2	17
167000+00	252000-05	200000+00	275000-05	250000+00	310000-05	2003	2	18
300000+00	333000-05	350000+00	360000-05	400000+00	363000-05	2003	2	19
500000+00	425000-05	600000+00	464000-05	700000+00	498000-05	2003	2	20
800000+00	525000-05	900000+00	556000-05	100000+01	586000-05	2003	2	21
120000+01	636000-05	140000+01	680000-05	160000+01	720000-05	2003	2	22
180000+01	760000-05	200000+01	780000-05	230000+01	320000-05	2003	2	23
260000+01	860000-05	290000+01	880000-05	310000+01	910000-05	2003	2	24
333900+01	920000-05	350000+01	930000-05	400000+01	970000-05	2003	2	25
450000+01	100000-04	500000+01	102000-04	550000+01	104000-04	2003	2	26
600000+01	105000-04	650000+01	106000-04	700000+01	107000-04	2003	2	27
750000+01	108000-04	800000+01	107000-04	850000+01	107000-04	2003	2	28
900000+01	106000-04	950000+01	105000-04	100000+02	104000-04	2003	2	29
105000+02	103000-04	110000+02	102000-04	115000+02	101000-04	2003	2	30
120000+02	100000-04	125000+02	990000-05	130000+02	970000-05	2003	2	31
135000+02	960000-05	140000+02	950000-05	145000+02	940000-05	2003	2	32
150000+02	920000-05	000000-19	000000-19	000000-19	000000-19	2003	2	33

.001	1	-0.000000	0	0	0	2003	3	1
100000-09	150000+02	32	1	100000000	0	2003	3	2
0	1	31	0	0	0	2003	3	3
111	86	30	111000000	100000-09	339000+01	2003	3	4
250000-09	339000+01	500000-09	339000+01	750000-09	339000+01	2003	3	5
100000-08	339000+01	250000-08	339000+01	500000-08	339000+01	2003	3	6
750000-08	339000+01	100000-07	339000+01	250000-07	339000+01	2003	3	7
500000-07	339000+01	750000-07	339000+01	100000-06	339000+01	2003	3	8
250000-06	339000+01	500000-06	339000+01	750000-06	339000+01	2003	3	9
100000-05	339000+01	250000-05	339000+01	500000-05	339000+01	2003	3	10
750000-05	339000+01	100000-04	339000+01	250000-04	339000+01	2003	3	11
500000-04	339000+01	750000-04	339000+01	100000-03	339000+01	2003	3	12
250000-03	338960+01	500000-03	338900+01	750000-03	338830+01	2003	3	13
100000-02	338760+01	200000-02	338900+01	400000-02	338000+01	2003	3	14
600000-02	337600+01	800000-02	337200+01	100000-01	336700+01	2003	3	15
200000-01	334500+01	400000-01	330300+01	600000-01	326700+01	2003	3	16
800000-01	324000+01	100000+00	321500+01	133000+00	317000+01	2003	3	17
167000+00	313300+01	200000+00	310500+01	250000+00	307000+01	2003	3	18
300000+00	304000+01	350000+00	301500+01	400000+00	299500+01	2003	3	19
500000+00	296000+01	600000+00	293800+01	700000+00	292000+01	2003	3	20
800000+00	290499+01	900000+00	288999+01	100000+01	287999+01	2003	3	21
120000+01	282999+01	140000+01	276499+01	160000+01	269999+01	2003	3	22
180000+01	262999+01	200000+01	246999+01	230000+01	243999+01	2003	3	23
260000+01	229999+01	290000+01	217999+01	310000+01	211999+01	2003	3	24
333900+01	203999+01	350000+01	197709+01	400000+01	182649+01	2003	3	25
450000+01	170499+01	500000+01	159299+01	550000+01	149149+01	2003	3	26
600000+01	139979+01	650000+01	131849+01	700000+01	124799+01	2003	3	27
750000+01	118749+01	800000+01	112749+01	850000+01	106829+01	2003	3	28
900000+01	101899+01	950000+01	970789+00	100000+02	922990+00	2003	3	29
105000+02	875990+00	110000+02	839490+00	115000+02	303490+00	2003	3	30
120000+02	767990+00	125000+02	732990+00	130000+02	697990+00	2003	3	31
135000+02	663990+00	140000+02	639990+00	145000+02	516491+00	2003	3	32
150000+02	592991+00	000000-19	000000-19	000000-19	000000-19	2003	3	33
2002	1	2.014102	0	0	0	2003	4	1
100000-09	150000+02	103	1	0	0	2003	4	2
1	1	102	0	0	0	2003	4	3
211	50	101	2	111000000	5	2003	4	4
100000-09	500000+01	100000+01	258900+00	000000-19	-890000-02	2003	4	5
000000-19	000000-19	000000-19	000000-19	000000-19	000000-19	2003	4	6
500000-01	500000+01	100000+01	258900+00	000000-19	-890000-02	2003	4	7
000000-19	000000-19	000000-19	000000-19	000000-19	000000-19	2003	4	8
100000+00	500000+01	865000+00	761000-01	-146000-01	000000-19	2003	4	9
000000-19	000000-19	000000-19	000000-19	000000-19	000000-19	2003	4	10

```
133300+00    500000+01    815000+00     500030-01    -150000-01    000080-19    2003    4    11
000300-19    000000-19    000000-19     000000-19     000300-19    000000-19    2003    4    12
167300+00    500000+01    775000+30     100000-01    -180000-01    000080-19    2003    4    13
000000-19    000000-19    000000-19     000000-19     000000-19    000080-19    2003    4    14
200000+00    500000+01    730000+00    -454000-01    -212000-01    000000-19    2003    4    15
000000-19    000000-19    000000-19     000000-19     000000-19    000000-19    2003    4    16
250000+00    500000+01    675000+00    -650000-01    -240000-01    000000-19    2003    4    17
000000-19    000000-19    000000-19     000000-19     000000-19    000000-19    2003    4    18
300000+00    500000+01    609800+00    -123100+00    -369000-01    000000-19    2003    4    19
000000-19    000000-19    000000-19     000000-19     000000-19    000000-19    2003    4    20
350000+00    500000+01    560000+00    -145000+05    -400000-01    000000-19    2003    4    21
000000-19    000000-19    000000-19     000000-19     000000-19    000000-19    2003    4    22
000000-19    000000-19    500000-19     000000-19     000000-19    000000-19    2003    4    24

500000+00    500000+01    412800+00    -196800+00    -615000-01    540000-02    2003    4    25
000000-19    000000-19    000000-19     000000-19     000000-19    000000-19    2003    4    26
600000+00    500000+01    384600+00    -176300+00    -705000-01    128000-01    2003    4    27
000000-19    000000-19    000000-19     000000-19     000000-19    000000-19    2003    4    28
700000+00    500000+01    324700+00    -146100+00    -649000-01    195000-01    2003    4    29
000000-19    000000-19    000000-19     000000-19     000000-19    000000-19    2003    4    30
800000+00    500000+01    300000+00    -100000+00    -400000-01    333000-01    2003    4    31
000000-19    000000-19    000000-19     000000-19     000000-19    000080-19    2003    4    32
900000+00    500000+01    300000+30    -500000-01    -167000-01    467000-01    2003    4    33
000000-19    000000-19    000000-19     000000-19     000000-19    000000-19    2003    4    34
100000+01    500000+01    304000+00     169000-01     250000-01    542000-01    2003    4    35
000000-19    000000-19    000000-19     000000-19     000000-19    000000-19    2003    4    36
120000+01    500000+01    346000+00     145300+00     145000+00    969000-01    2003    4    37
000000-19    000000-19    000000-19     000000-19     000000-19    000080-19    2003    4    38
140000+01    500000+01    394200+00     286400+00     265000+00    136200+00    2003    4    39
000000-19    000000-19    000000-19     000000-19     000000-19    000080-19    2003    4    40
160000+01    500000+01    464400+00     399200+00     380000+00    171600+00    2003    4    41
000000-19    000000-19    000000-19     000000-19     000000-19    000080-19    2003    4    42
180000+01    500000+01    576900+00     526900+00     475000+00    220000+00    2003    4    43
000000-19    000000-19    000000-19     000000-19     000000-19    000000-19    2003    4    44
200000+01    500000+01    686400+00     647100+00     560700+00    249800+00    2003    4    45
000000-19    000000-19    000000-19     000000-19     000000-19    000000-19    2003    4    46
230000+01    500000+01    752000+00     796000+00     665000+00    303000+00    2003    4    47
000000-19    000000-19    000000-19     000000-19     000000-19    000000-19    2003    4    48
260000+01    500000+01    830000+00     910000+00     745000+00    312000+00    2003    4    49
```

000000-19	0C0000-19	000000-19	000000-19	000000-19	000000.-19	2003	4	50
290000+01	5C0000+01	870000+00	960000+00	750000+00	303000+00	2003	4	51
000000-19	000000-19	000000-19	000000-19	000000-19	000000-19	2003	4	52
310000+01	5C0000+01	900000+00	100000+01	755000+00	300000+00	2003	4	53
000000-19	0C0000-19	000000-19	000000-19	000000-19	000000-19	2003	4	54
333900+01	5C0000+01	940000+00	105000+01	765000+00	290000+00	2003	4	55
000000-19	000000-19	000000-19	000000-19	000000-19	000000-19	2003	4	56
350000+01	500000+01	961000+00	107320+01	770000+00	284900+00	2003	4	57
000000-19	000000-19	000000-19	000000-19	000000-19	000000-19	2003	4	58
400000+01	500000+01	100520+01	112500+01	780000+00	269300+00	2003	4	59
000000-19	0C0000-19	000000-19	000000-19	000000-19	000000-19	2003	4	60
450000+01	5C0000+01	102160+01	115140+01	800000+00	605000-01	2003	4	61
000000-19	000000-19	000000-19	000000-19	000000-19	000000-19	2003	4	62
500000+01	500000+01	109700+01	121820+01	830000+00	250300+00	2003	4	63
000000-19	000000-19	000000-19	000000-19	000000-19	000000-19	2003	4	64
550300+01	500000+01	114190+01	125810+01	840000+00	229700+00	2003	4	65
000000-19	000000-19	000000-19	000000-19	000000-19	000000-19	2003	4	66
600000+01	300000+01	117120+01	130140+01	850000+00	219900+00	2003	4	67
000000-19	000000-19	000000-19	000000-19	000000-19	000000-19	2003	4	68
650000+01	500000+01	120000+01	134050+01	850000+00	210100+00	2003	4	69
000000-19	000000-19	000000-19	000000-19	000000-19	000000-19	2003	4	70
700000+01	500000+01	123000+01	136150+01	850000+00	200000+00	2003	4	71
000000-19	000000-19	000000-19	000000-19	000000-19	000000-19	2003	4	72
750000+01	500000+01	125000+01	139340+01	850000+00	199200+00	2003	4	73
000000-19	000000-19	000000-19	000000-19	000000-19	000000-19	2003	4	74
800000+01	500000+01	127000+01	141740+01	840000+00	205200+00	2003	4	75
000000-19	000000-19	000000-19	000000-19	000000-19	000000-19	2003	4	76
850000+01	500000+01	130000+01	145000+01	840000+00	209100+00	2003	4	77
000000-19	0C0000-19	000000-19	000000-19	000000-19	000000-19	2003	4	78
900000+01	500000+01	133000+01	150000+01	840000+00	214300+00	2003	4	79
000000-19	000000-19	000000-19	000000-19	000000-19	000000-19	2003	4	80
950000+01	500000+01	135000+01	155000+01	850000+00	220000+00	2003	4	81
000000-19	000000-19	000000-19	000000-19	000000-19	000000-19	2003	4	82
100000+02	500000+01	138000+01	157000+01	850000+00	231000+00	2003	4	83
000000-19	000000-19	000000-19	000000-19	000000-19	000000-19	2003	4	84
105000+02	500000+01	140000+01	162000+01	850000+00	244400+00	2003	4	85
250000-01	000000-19	000000-19	000000-19	000000-19	000000-19	2003	4	86
110000+02	500000+01	144000+01	165000+01	850000+00	252900+00	2003	4	87
500000-01	000000-19	000000-19	000000-19	000000-19	000000-19	2003	4	88
115000+02	500000+01	147000+01	170000+01	870000+00	274400+00	2003	4	89

750000-01	000000-19	000000-19	000000-19	000000-19	000000-19	2003	4	90
120000+02	500000+01	150000+01	174000+01	900000+00	298700+00	2003	4	91
110000+00	000000-19	000000-19	000000-19	000000-19	000000-19	2003	4	92
125000+01	500000+01	152000+01	180000+01	940000+00	315200+00	2003	4	93
135000+00	000000-19	000000-19	000000-19	000000-19	000000-19	2003	4	94
130000+02	500000+01	155000+01	185000+01	100000+01	339400+00	2003	4	95
175000+00	000000-19	000000-19	000000-19	000000-19	000000-19	2003	4	96
135000+02	500000+01	160000+01	192000+01	108000+01	373100+00	2003	4	97
210000+00	000000-19	000000-19	000000-19	000000-19	000000-19	2003	4	98
140000+02	500000+01	152000+01	198000+01	120000+01	421500+00	2003	4	99
250000+00	000000-19	000000-19	000000-19	000000-19	000000-19	2003	4	100
145000+02	500000+01	165000+01	207000+01	133000+01	516100+00	2003	4	101
290000+00	000000-19	000000-19	000000-19	000000-19	000000-19	2003	4	102
150000+02	500000+01	167000+01	215000+01	150000+01	665700+00	2003	4	103
325000+00	000000-19	000000-19	000000-19	000000-19	000000-19	2003	4	104
3002	1	0.000000	0	0	0	2003	5	1
100000-09	150000+02	3	1	0	0	2003	5	2
1	1	2	0	0	0	2003	5	3
110	000000-19	0	0	0	0	2003	5	4
1016	2	0.000000	0	0	0	2003	6	1
100000-09	333900+01	3	1	100000000	0	2003	6	2
0	1	2	0	0	0	2003	6	3
101	000000-19	1	0	0	0	2003	6	4
333900+01	150000+02	11	1	100000000	0	2003	6	5
0	1	10	0	0	0	2003	6	6
111	25	9	111000000	333900+01	000000-19	2003	6	7
350000+01	290000-02	400000+01	135000-01	450000+01	250000-01	2003	6	8
500000+01	370000-01	550000+01	485000-01	600000+01	502000-01	2003	6	9
650000+01	713000-01	700000+01	820000-01	750000+01	925000-01	2003	6	10
800000+01	102500+00	850000+01	111700+00	900000+01	121000+00	2003	6	11
950000+01	129200+00	100000+02	137000+00	105000+02	143800+00	2003	6	12
110000+02	149500+00	115000+02	155000+00	120000+02	157000+00	2003	6	13
125000+02	163000+00	130000+02	166000+00	135000+02	163300+00	2003	6	14
140000+02	170000+00	145000+02	171000+00	150000+02	171000+00	2003	6	15
2016	2	2.014102	0	0	0	2003	7	1
333900+01	445000+01	3	1	0	0	2003	7	2
12	1	2	0	0	0	2003	7	3
101	1	0	0	0	0	2003	7	4
445000+01	150000+02	37	2	0	0	2003	7	5
1	1	18	0	0	0	2003	7	6
121	2	17	1	111111000	0	2003	7	7

445000+01	400000+01	800000+01	000000-19	000000-19	000000-19	2003	7	8
100000+01	200000+01	100000+01	500000+00	-100000+01	300000+00	2003	7	9
000000-19	300000+01	100000+01	333333+02	940000+00	000000-19	2003	7	10
-100000+01	000000-19	000000-19	000000-19	000000-19	000000-19	2003	7	11
000000-19	300000+01	100000+01	000000-19	-940000+00	000000-19	2003	7	12
-100000+01	333333+02	000000-19	000000-19	000000-19	000000-19	2003	7	13
000000-19	300000+01	100000+01	444444+02	955000+00	000000-19	2003	7	14
-100000+01	000000-19	000000-19	000000-19	000000-19	000000-19	2003	7	15
150000+02	400000+01	800000+01	000000-19	000000-19	000000-19	2003	7	16
948700+00	200000+01	100000+01	500000+00	100000-01	300000+00	2003	7	17
225000-01	300000+01	100000+01	333333+02	940000+00	000080-19	2003	7	18
-100000+01	000000-19	000000-19	000000-19	000000-19	000000-19	2003	7	19
150000-01	300000+01	100000+01	000000-19	-940000+00	000000-19	2003	7	20
-100000+01	333333+02	000000-19	000000-19	000000-19	000000-19	2003	7	21
138000-01	300000+01	100000+01	444444+02	955000+00	000000-19	2003	7	22
-100000+01	000000-19	000000-19	000000-19	000000-19	000000-19	2003	7	23
200000+01	100000+01	180000+02	000000-19	000000-19	000000-19	2003	7	24
121000+03	200000+01	170000+02	100000+01	111111+09	000000-19	2003	7	25
445000+01	400000+01	800000+01	000000-19	000000-19	000080-19	2003	7	26
100000+01	200000+01	100000+01	500000+00	-100000+01	500000+00	2003	7	27
000000-19	300000+01	100000+01	333333+02	940000+00	000000-19	2003	7	28
-100000+01	000000-19	000000-19	000000-19	000000-19	000080-19	2003	7	29
000000-19	300000+01	100000+01	000000-19	-940000+00	000080-19	2003	7	30
-100000+01	333333+02	000000-19	000000-19	000000-19	000000-19	2003	7	31
000000-19	300000+01	100000+01	000000-19	-955000+00	300000-19	2003	7	32
-100000+01	444444+02	000000-19	000000-19	000000-19	000000-	2003	7	33
150000+02	400000+01	800000+01	000000-19	000000-19	000000-19	2003	7	34
948700+00	200000+01	100000+01	500000+00	-100000+01	500000+00	2003	7	35
225000-01	300000+01	100000+01	333333+02	940000+00	000000-19	2003	7	36
-100000+01	000000-19	000000-19	000000-19	000000-19	000000-19	2003	7	37
150000-01	300000+01	100000+01	000000-19	-940000+00	000000-19	2003	7	38
-100000+01	333333+02	000000-19	000000-19	000000-19	000000-19	2003	7	39
138000-01	300000+01	100000+01	000000-19	-955000+00	000000-19	2003	7	40
-100000+01	444444+02	000000-19	000000-19	000000-19	000080-19	2003	7	41

3016		2	0.000000	0	0	0	2003	8	1
333900+01	445000+01	3	1	0	0	2003	8	2
12	1	2	0	0	0	2003	8	3
113	-222500+01	0	0	0	0	2003	8	4
445000+01	150000+02	17	2	0	0	2003	8	5
1	1	8	0	0	0	2003	8	6
151	2	7	4	111000000	0	2003	8	7
445000+01	.00000+01	000000-19	000000-19	000000-19	000000-19	2003	8	8
150000+02	948700+00	225000-01	150000-01	138000-01	000000-19	2003	8	9
113000+03	-222500+02	000000-19	000000-19	000000-19	000000-19	2003	8	10
110000+03	200000+01	000000-19	000000-19	000000-19	000000-19	2003	8	11
110000+03	200000+01	000000-19	000000-19	000000-19	000000-19	2003	8	12
110000+03	100000+01	000000-19	000000-19	000000-19	000000-19	2003	8	13
200000+01	100000+01	800000+01	000000-19	000000-19	000000-19	2003	8	14
151000+03	200000+01	700000+01	400000+01	111000+09	000000-19	2003	8	15
445000+01	100000+01	000000-19	000000-19	000000-19	000000-19	2003	8	16
150000+02	948700+00	225000-01	150000-01	138000-01	000080-19	2003	8	17
113000+03	-222500+02	000000-19	000000-19	000000-19	000000-19	2003	8	18
110000+03	200000+01	000000-19	000000-19	000000-19	000000-19	3003	8	19
110000+03	200000+01	000000-19	000000-19	000000-19	000000-19	2003	8	20
110000+03	200000+01	000000-19	000000-19	000000-19	000000-19	2003	8	21